LHCb fixed-target results and prospects

L. L. Pappalardo
(on behalf of the LHCb Collaboration)

The 18th International Conference on Strangeness on Quark Matter (SQM 2019)

The LHCb fixed-target system SMOG

The LHCb detector

- A single-arm spectrometer designed for the study of particles containing c or b quarks
- **Forward acceptance**: $2 < \eta < 5$

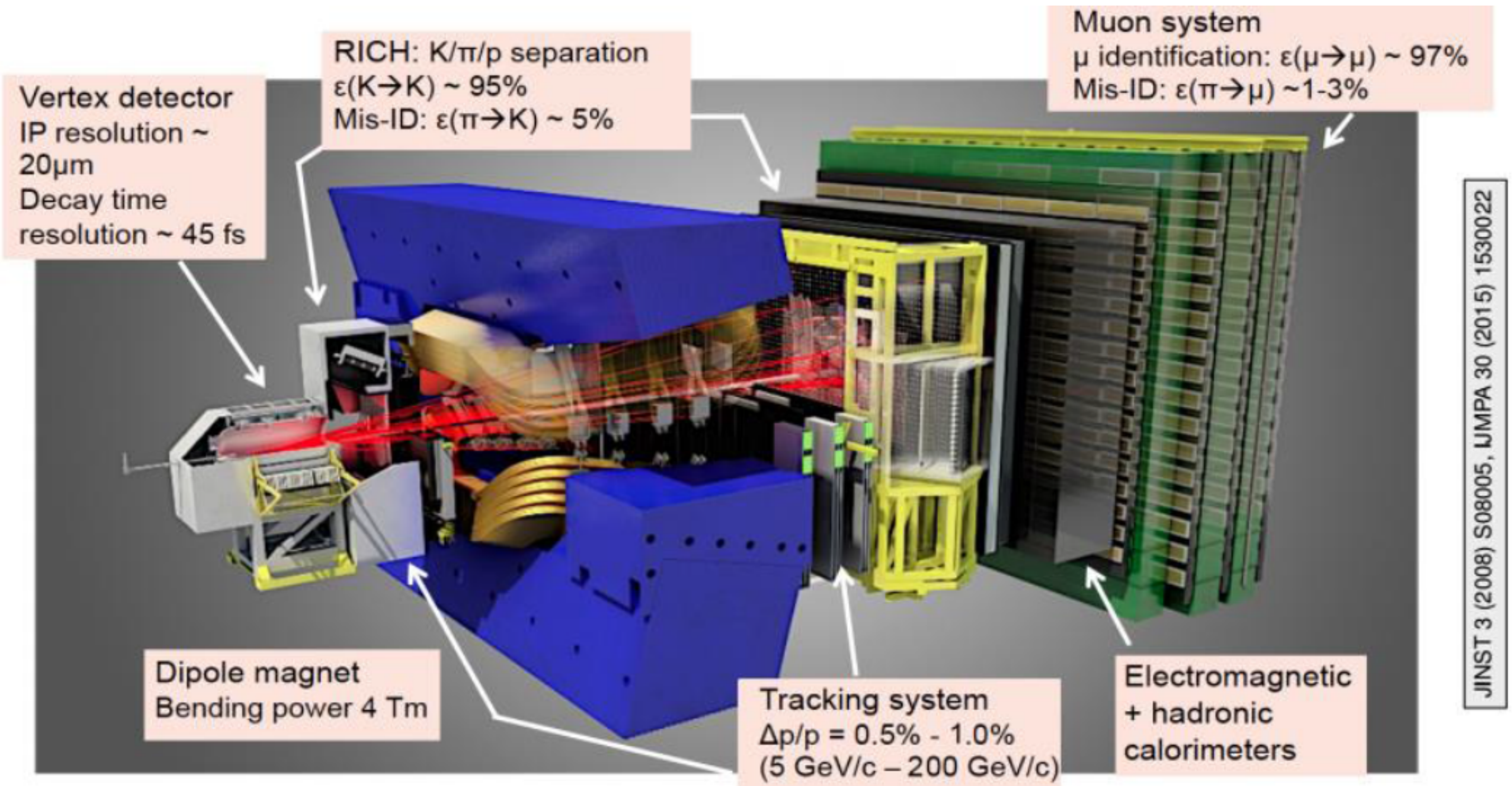

The LHCb detector

- A single-arm spectrometer designed for the study of particles containing c or b quarks
- **Forward acceptance:** $2 < \eta < 5$

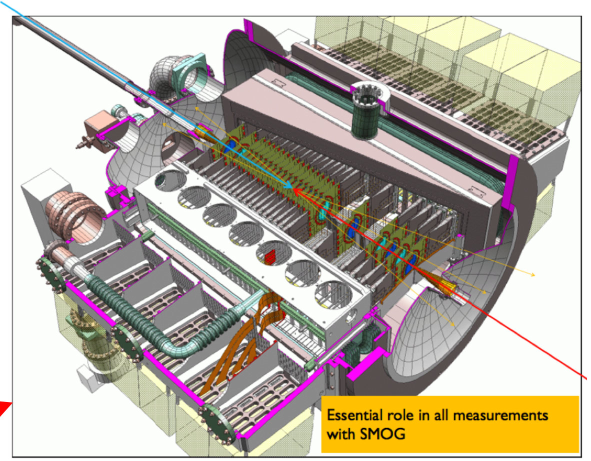

VELO vessel

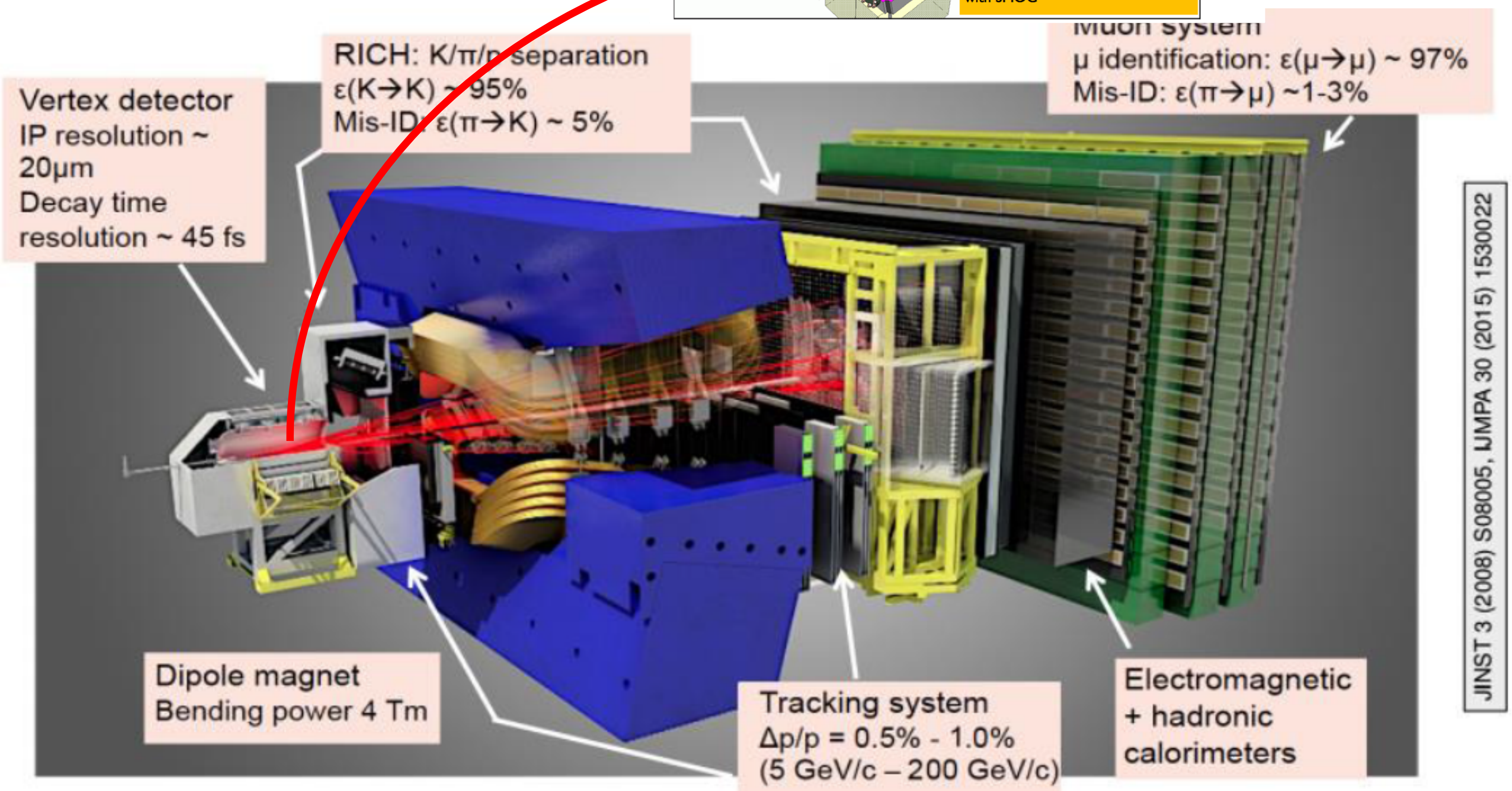

The LHCb fixed-target system

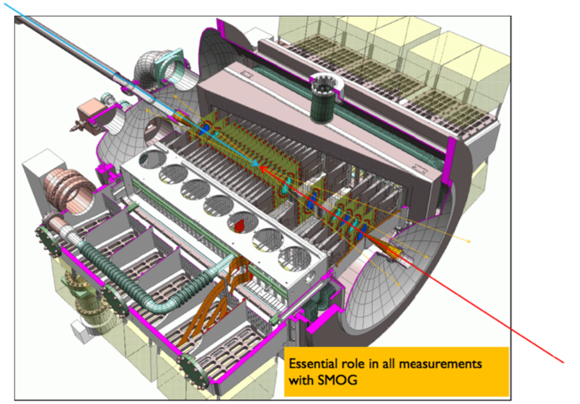

SMOG: System for Measuring Overlap with Gas:

- Low density noble gas injected in the VELO vessel ($\sim 10^{-7}$mbar)
- Gas pressure 2 orders of magnitude higher than LHC vacuum
- Beam-gas collision rate increased by 2 orders of magnitude

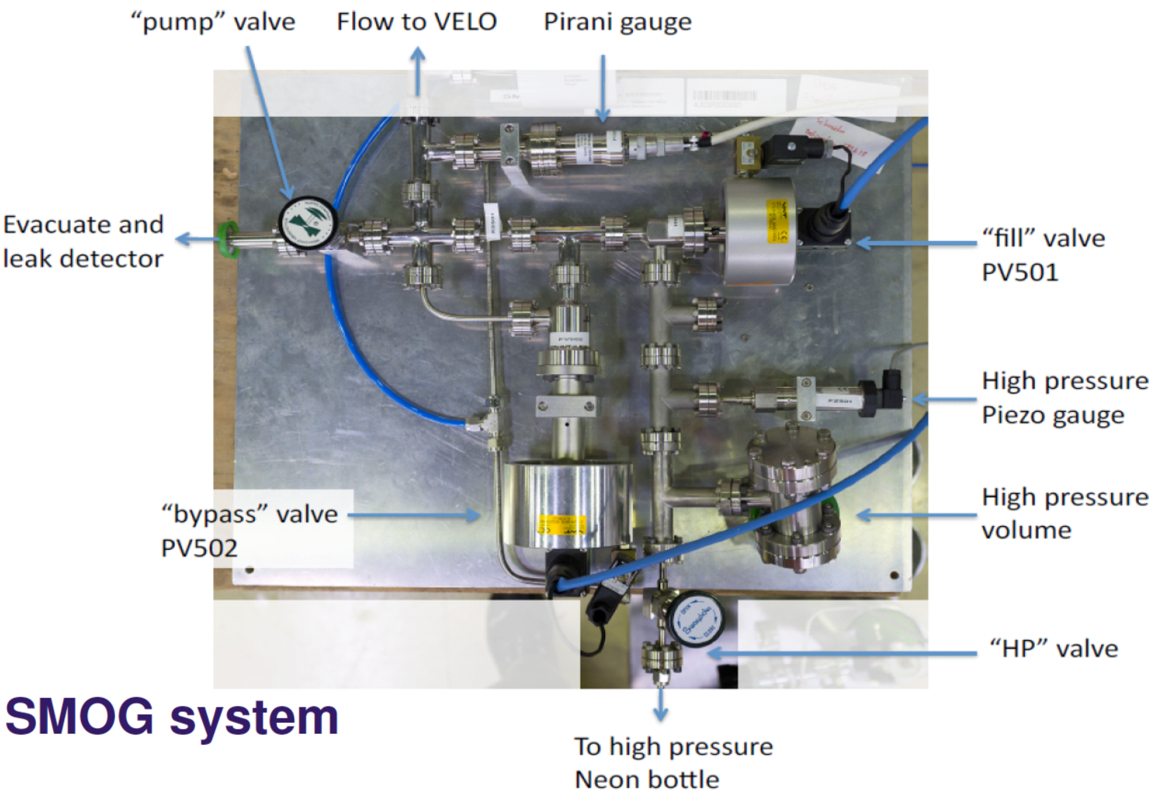

SMOG system

The LHCb fixed-target system

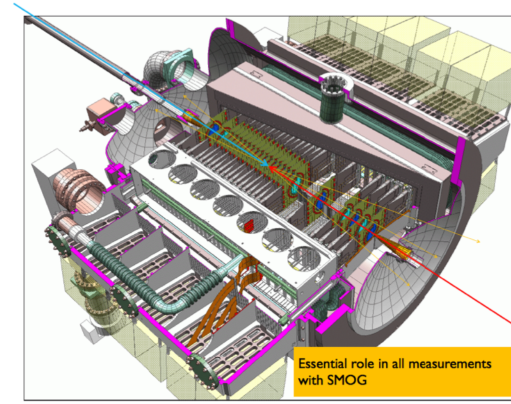

SMOG: System for Measuring Overlap with Gas:

- Low density noble gas injected in the VELO vessel ($\sim 10^{-7}$mbar)
- Gas pressure 2 orders of magnitude higher than LHC vacuum
- Beam-gas collision rate increased by 2 orders of magnitude
- Conceived for **precise luminosity determination** (beam-gas imaging)

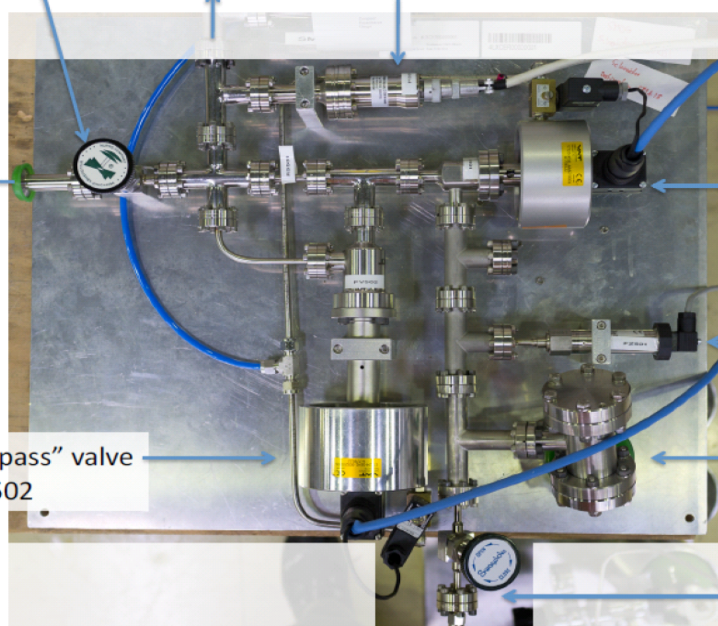

SMOG system

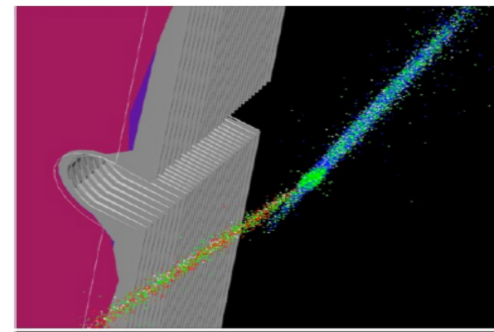

Distribution of vertices overlaid on detector display. z-axis is scaled by 1:100 compared to transverse dimensions to see the beam angle.
Beam 1 - Beam 2, Beam 1 - Gas, Beam 2 - Gas.

The LHCb fixed-target system

SMOG: System for Measuring Overlap with Gas:

- Low density noble gas injected in the VELO vessel ($\sim 10^{-7}$ mbar)
- Gas pressure 2 orders of magnitude higher than LHC vacuum
- Beam-gas collision rate increased by 2 orders of magnitude
- Conceived for **precise luminosity determination** (beam-gas imaging)

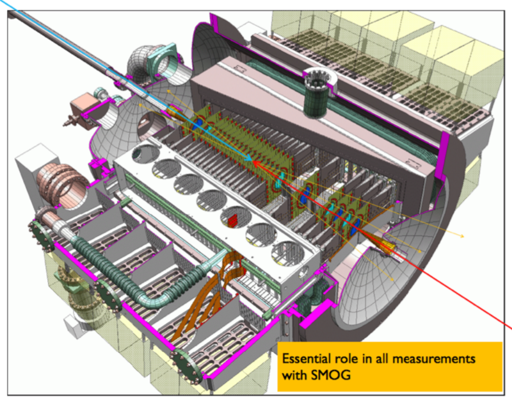

…but SMOG gives also the unique opportunity to operate an **LHC experiment in a fixed-target mode** and to study pA and AA collisions on various targets!

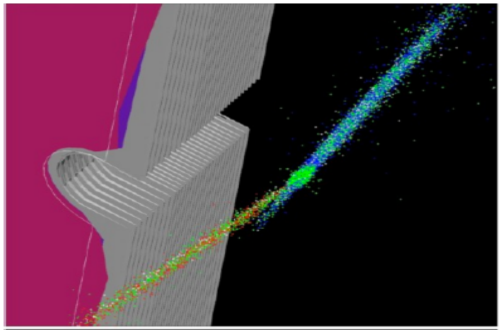

Distribution of vertices overlaid on detector display. z-axis is scaled by 1:100 compared to transverse dimensions to see the beam angle.
Beam 1 - Beam 2, Beam 1 - Gas, Beam 2 - Gas.

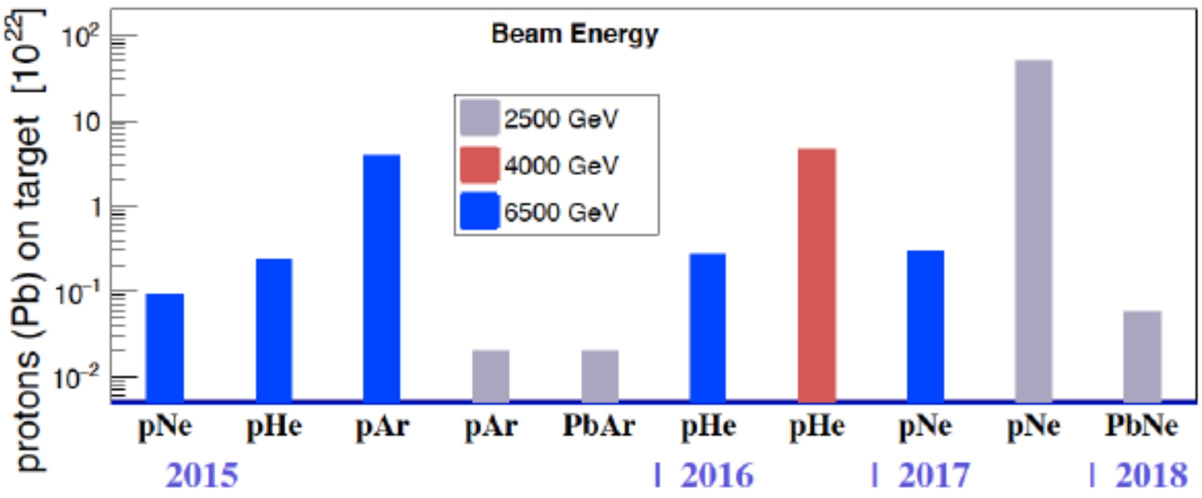

Kinematic conditions for fixed-target collisions at LHC

$E_p = 7$ TeV ⟹ $\gamma = \frac{\sqrt{s}}{2m_p} \approx 60$ **CM strongly boosted in the lab system!**

Kinematic conditions for fixed-target collisions at LHC

$E_p = 7$ TeV $\Rightarrow$ $\gamma = \frac{\sqrt{s}}{2m_p} \approx 60$ **CM strongly boosted in the lab system!**

LHCb acceptance
$(2 \lesssim y_{lab} \lesssim 5)$ $\Leftrightarrow$ $-3.0 \lesssim y^* \lesssim 0$ **CM backward rapidity region**

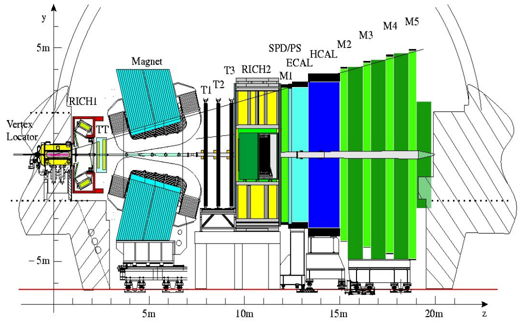

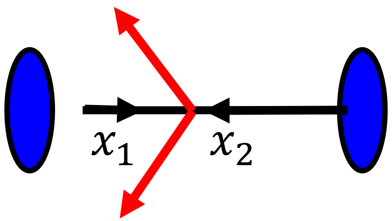

Kinematic conditions for fixed-target collisions at LHC

$E_p = 7$ TeV ⟹ $\gamma = \frac{\sqrt{s}}{2m_p} \approx 60$ **CM strongly boosted in the lab system!**

LHCb acceptance
$(2 \lesssim y_{lab} \lesssim 5)$ ⟺ $-3.0 \lesssim y^* \lesssim 0$ **CM backward rapidity region**

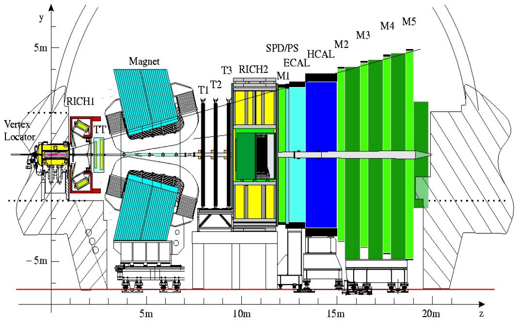

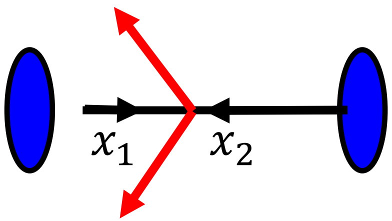

Few-Body Syst (2017) 58: 139

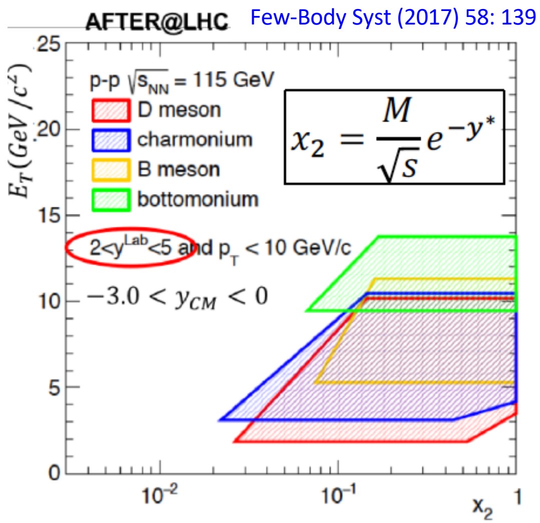

Kinematic conditions for fixed-target collisions at LHC

$E_p = 7$ TeV ➡ $\gamma = \dfrac{\sqrt{s}}{2m_p} \approx 60$ **CM strongly boosted in the lab system!**

LHCb acceptance
$(2 \lesssim y_{lab} \lesssim 5)$ ⟷ $-3.0 \lesssim y^* \lesssim 0$ **CM backward rapidity region**

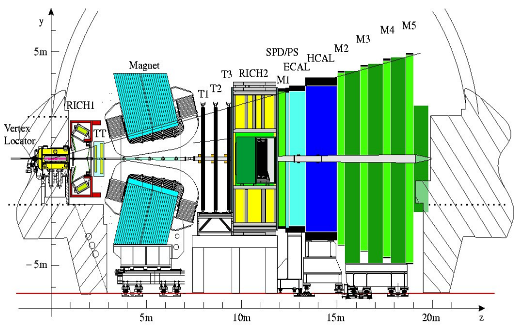

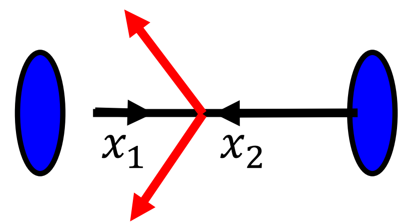

Few-Body Syst (2017) 58: 139

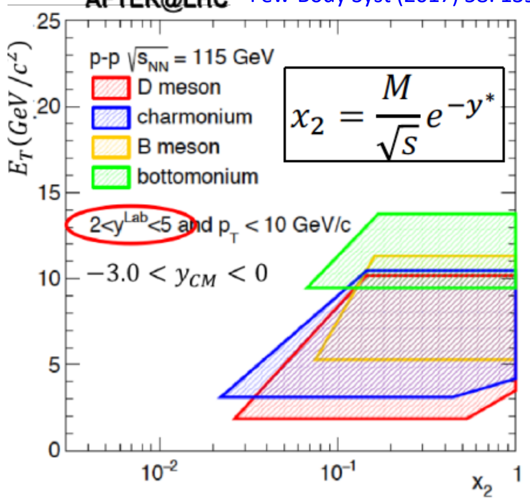

[R. D. Ball et al. Eur. Phys. J. C76 (2016) 383]

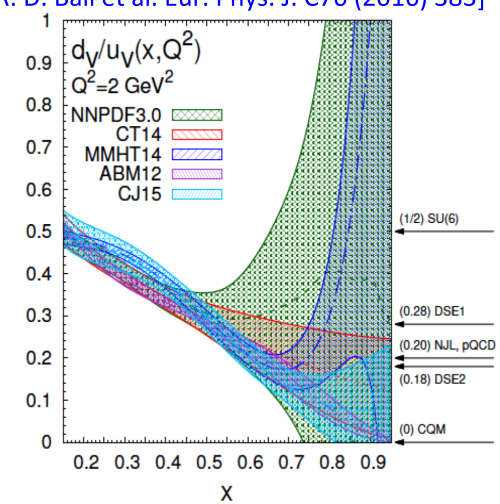

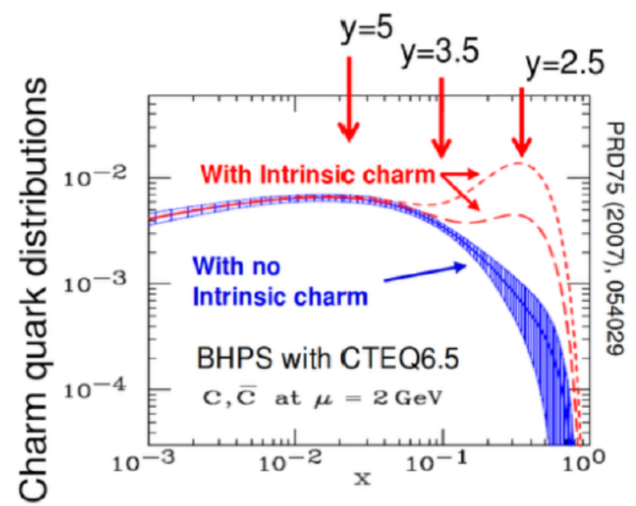

First physics results with SMOG

- Prompt charm production in p-He and p-Ar collisions

Physics motivations

Heavy quarks are effective probes to study the properties of the deconfined medium created in **ultra-relativistic heavy-ion collisions:**

- Their masses are significantly higher than the QGP critical temperature ($T_c \sim 156$ MeV)
- They are **produced in the early stages of the collision** in a time scale that is shorter than that of the QGP formation

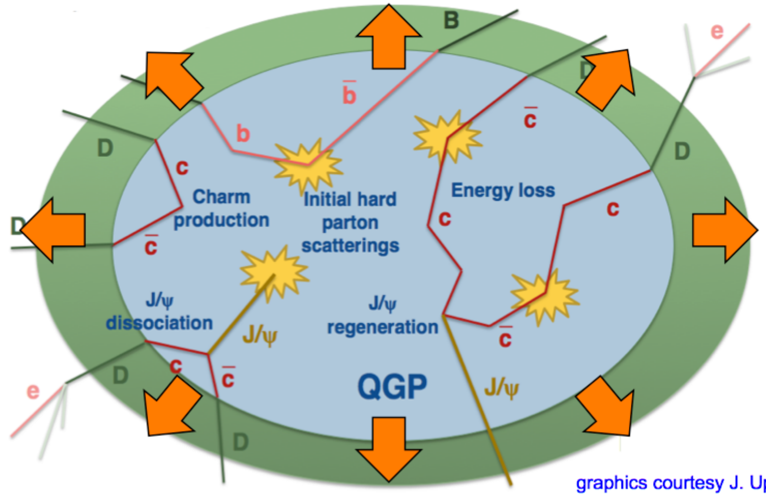

graphics courtesy J. Uphoff

Physics motivations

Heavy quarks are effective probes to study the properties of the deconfined medium created in **ultra-relativistic heavy-ion collisions:**

- Their masses are significantly higher than the QGP critical temperature ($T_c \sim 156$ MeV)
- They are **produced in the early stages of the collision** in a time scale that is shorter than that of the QGP formation

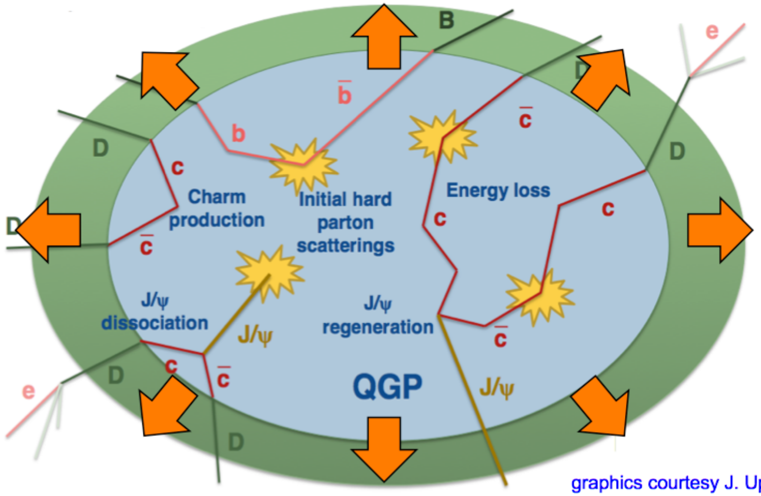

graphics courtesy J. Uphoff

Extracted from arXiv:1212,1701

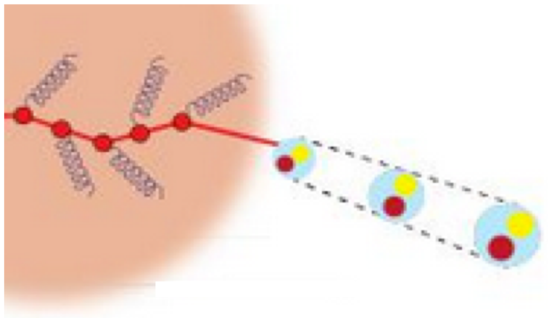

While crossing the dense medium, quarks loose energy via **radiative gluonic emissions** and **collisions** with the medium constituents.

Studying these **re-scatterings and energy loss processes** is of outmost importance for understanding the properties of the formed QGP and its space-time evolution!

Physics motivations

A correct interpretation of these processes in terms of QGP formation, requires a full understanding of the **cold-nuclear-matter effects:**

- Initial-state radiation or energy-loss
- Final-state hadronic rescattering and absorption
- **Modification of the nucleon PDFs in nuclear matter**

Physics motivations

A correct interpretation of these processes in terms of QGP formation, requires a full understanding of the **cold-nuclear-matter effects:**

- Initial-state radiation or energy-loss
- Final-state hadronic rescattering and absorption
- **Modification of the nucleon PDFs in nuclear matter**

$$R_i^A(x,Q^2) = \frac{f_i^{p/A}(x,Q^2)}{f_i^{p}(x,Q^2)}$$

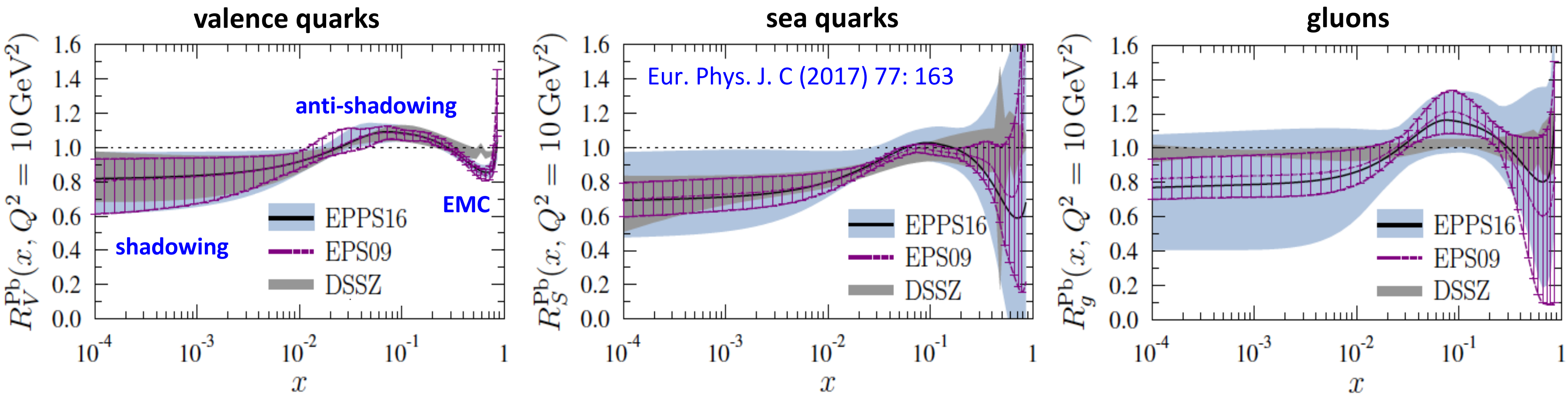

Physics motivations

A correct interpretation of these processes in terms of QGP formation, requires a full understanding of the **cold-nuclear-matter effects:**

- Initial-state radiation or energy-loss
- Final-state hadronic rescattering and absorption
- **Modification of the nucleon PDFs in nuclear matter**

$$R_i^A(x,Q^2) = \frac{f_i^{p/A}(x,Q^2)}{f_i^{p}(x,Q^2)}$$

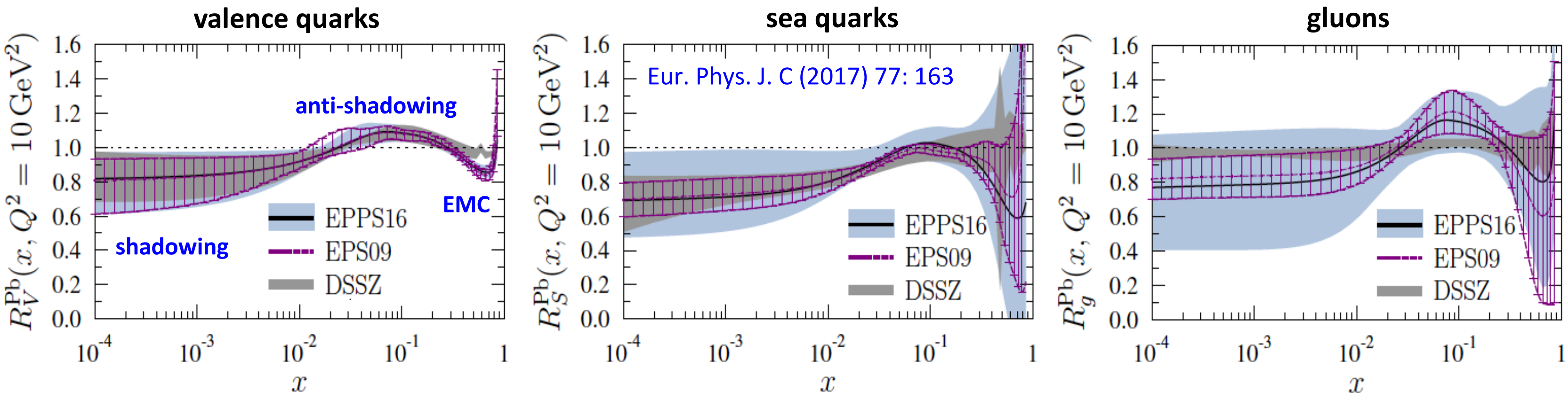

Measurements of prompt heavy-quark production in fixed-target pA collisions at LHC allow to:

- ➢ constraint nPDFs at high-x (anti-shadowing, EMC effect)
- ➢ pin-down possible contributions from intrinsic charm, expected at high-x
- ➢ better understand the charmonium suppression mechanisms observed in heavy-ion collisions
- ➢ study the charmonium production mechanisms in a QGP-free environment

Prompt charm production in p-He and p-Ar collisions

LHCb recently reported the first measurement of J/ψ **and** D^0 **production** in fixed-target configuration using **p-He** and **p-Ar** collisions with SMOG

$\sqrt{s_{NN}} = 110$ GeV

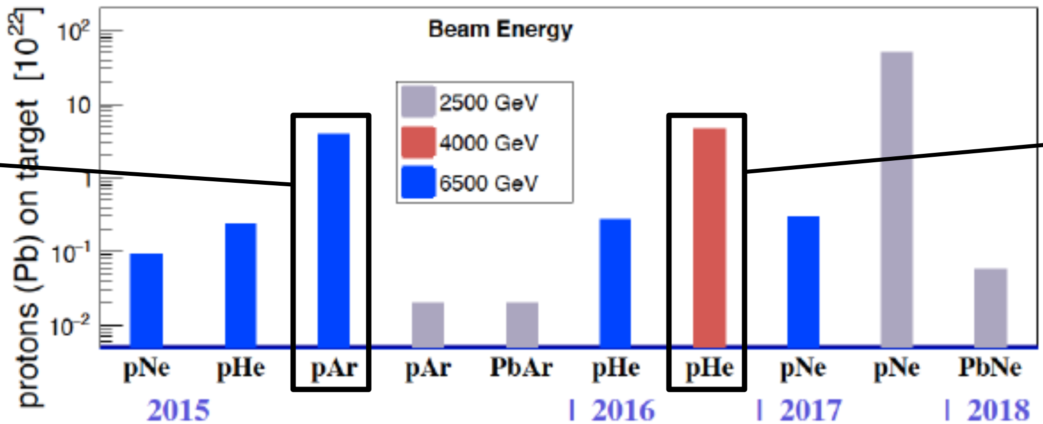

$\sqrt{s_{NN}} = 87$ GeV

Prompt charm production in p-He and p-Ar collisions

LHCb recently reported the first measurement of $\boldsymbol{J/\psi}$ **and** $\boldsymbol{D^0}$ **production** in fixed-target configuration using **p-He** and **p-Ar** collisions with SMOG

$\sqrt{s_{NN}} = 110$ GeV

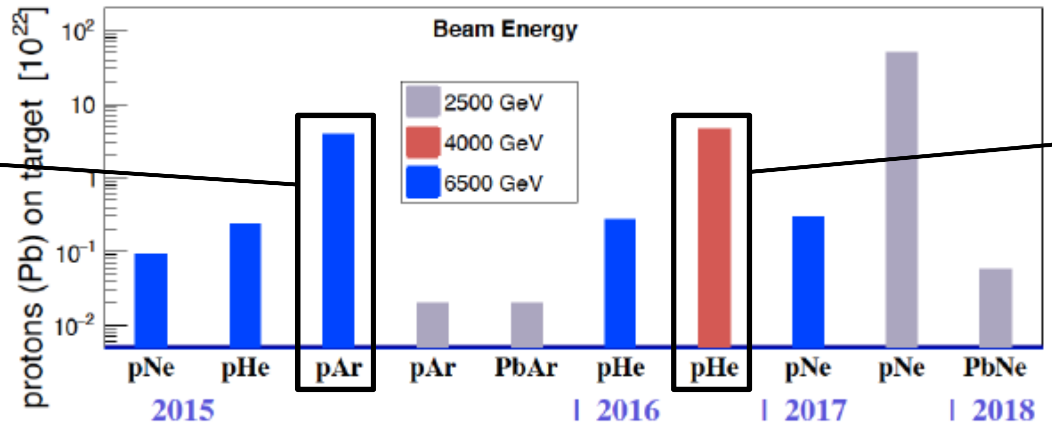

$\sqrt{s_{NN}} = 87$ GeV

- **Prompt** $\boldsymbol{J/\psi}$ **and** $\boldsymbol{D^0}$ **signal yields** are obtained in an unbinned ML fit of the invariant mass distributions using $J/\psi \to \mu^+\mu^-$ and $D^0 \to K\pi$

Phys. Rev. Lett. 122, 132002 (2019)

Sig: CB
Bkg: exp

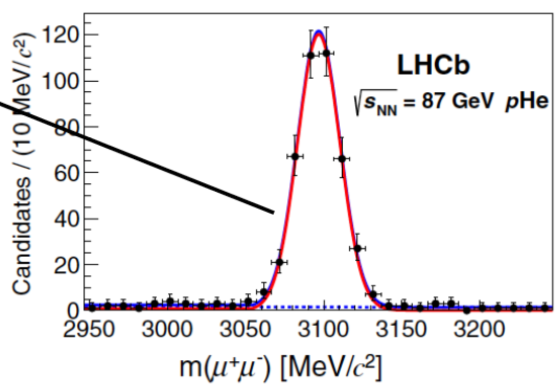

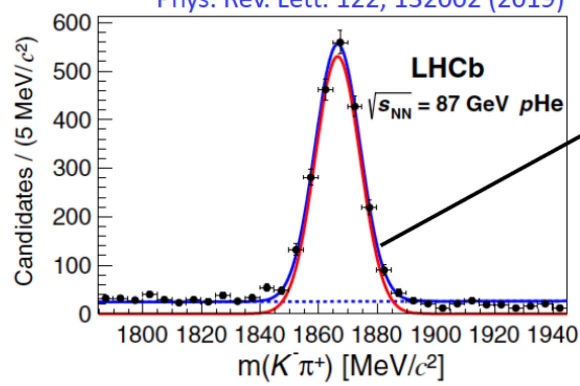

Sig: 2 Gauss
Bkg: exp

Prompt charm production in p-He collisions at $\sqrt{s} = 87$ GeV

Luminosity determined from yield of electrons elastically scattered off target He atoms:

$\mathcal{L}_{pHe} = 7.58 \pm 0.47\ \text{nb}^{-1}$ (not available for the Ar-target data)

Prompt charm production in p-He collisions at $\sqrt{s} = 87$ GeV

Luminosity determined from yield of electrons elastically scattered off target He atoms:

$$\mathcal{L}_{pHe} = 7.58 \pm 0.47\ \text{nb}^{-1}$$ (not available for the Ar-target data)

Integrated cross-sections

$$\left.\begin{aligned} \sigma_{J/\psi} &= 652 \pm 33(\text{stat}) \pm 42(syst)\quad \text{nb/nucleon} \\ \sigma_{D^0} &= 80.8 \pm 2.4(\text{stat}) \pm 6.3(syst)\quad \text{nb/nucleon} \end{aligned}\right\} y \in [2.0, 4.6]$$

Prompt charm production in p-He collisions at $\sqrt{s} = 87$ GeV

Luminosity determined from yield of electrons elastically scattered off target He atoms:

$$\mathcal{L}_{pHe} = 7.58 \pm 0.47 \text{ nb}^{-1}$$ (not available for the Ar-target data)

Integrated cross-sections

$$\sigma_{J/\psi} = 652 \pm 33(\text{stat}) \pm 42(syst) \quad \text{nb/nucleon}$$
$$\sigma_{D^0} = 80.8 \pm 2.4(\text{stat}) \pm 6.3(syst) \quad \text{nb/nucleon}$$
$y \in [2.0, 4.6]$

Extrapolated to full phase-space (using PYTHIA8)

$$\sigma_{J/\psi} = 1225.6 \pm 100.7 \quad \text{nb/nucleon}$$

$$\sigma_{D^0} = 156.0 \pm 13.1 \quad \text{nb/nucleon}$$

Phys. Rev. Lett. 122, 132002 (2019)

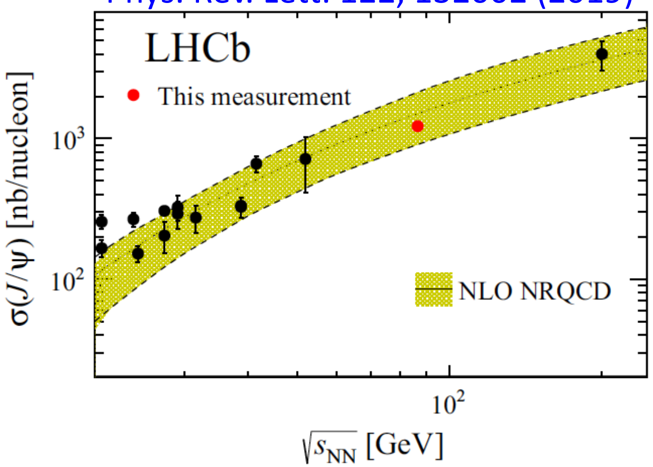

Prompt charm production in p-He collisions at $\sqrt{s} = 87$ GeV

Luminosity determined from yield of electrons elastically scattered off target He atoms:

$$\mathcal{L}_{pHe} = 7.58 \pm 0.47 \text{ nb}^{-1}$$ (not available for the Ar-target data)

Integrated cross-sections

$$\left.\begin{aligned} \sigma_{J/\psi} &= 652 \pm 33(\text{stat}) \pm 42(syst) \quad \text{nb/nucleon} \\ \sigma_{D^0} &= 80.8 \pm 2.4(\text{stat}) \pm 6.3(syst) \quad \text{nb/nucleon} \end{aligned}\right\} y \in [2.0, 4.6]$$

Extrapolated to full phase-space (using PYTHIA8)

$$\sigma_{J/\psi} = 1225.6 \pm 100.7 \quad \text{nb/nucleon}$$

$$\sigma_{D^0} = 156.0 \pm 13.1 \text{ nb/nucleon}$$ → scaled with global $f(c \to D^0)$ FF to obtain the $c\bar{c}$ production cross section:

$$\sigma_{c\bar{c}} = 288.0 \pm 24.2 \pm 6.9 \quad \text{nb/nucleon}$$

Phys. Rev. Lett. 122, 132002 (2019)

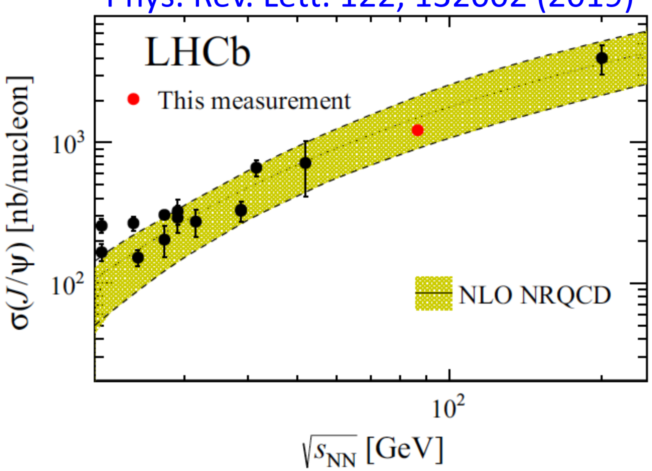

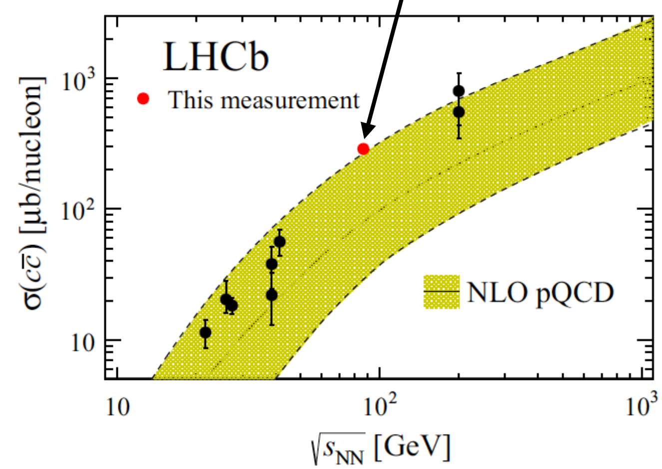

Prompt charm production in p-He collisions at $\sqrt{s} = 87$ GeV

Phys. Rev. Lett. 122, 132002 (2019)

J/ψ

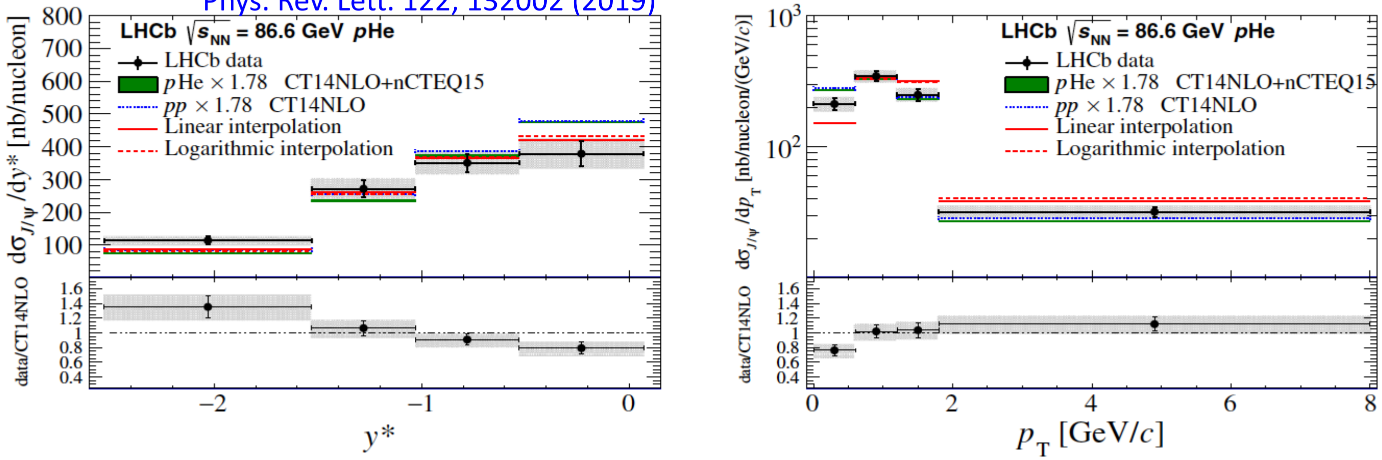

HELAC-ONIA predictions:
- JHEP 1303 (2013) 122
- Eur. Phys. J. C 77, 1 (2017)
- Comput. Phys. Commun. 198, 238 (2016)

Phenom. models:
- JHEP 1303 (2013) 122
- JHEP 05 (2013) 155

Prompt charm production in p-He collisions at $\sqrt{s} = 87$ GeV

Phys. Rev. Lett. 122, 132002 (2019)

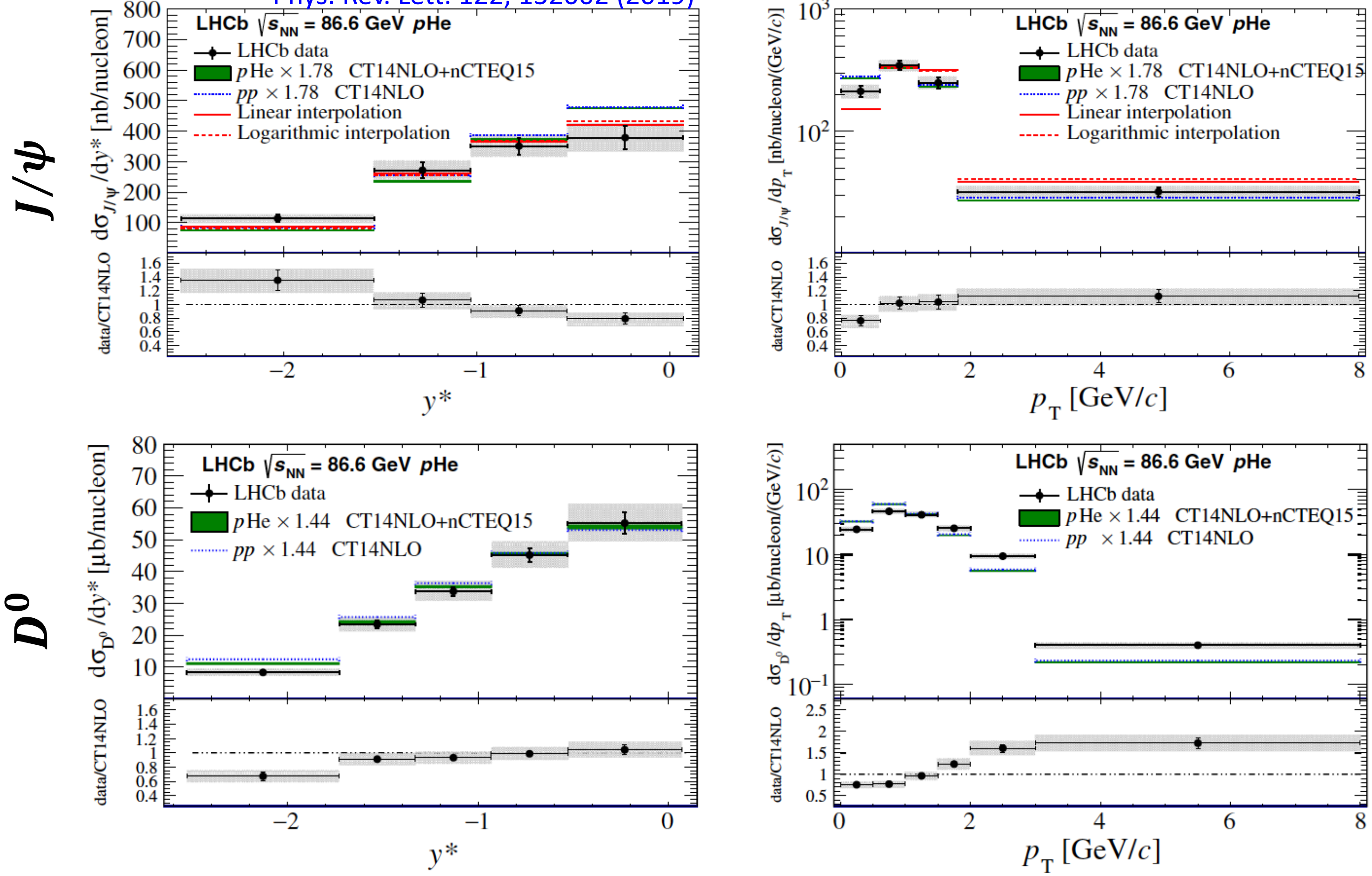

HELAC-ONIA predictions:

- JHEP 1303 (2013) 122
- Eur. Phys. J. C 77, 1 (2017)
- Comput. Phys. Commun. 198, 238 (2016)

Phenom. models:

- JHEP 1303 (2013) 122
- JHEP 05 (2013) 155

Prompt charm production in p-He collisions at $\sqrt{s} = 87$ GeV

Phys. Rev. Lett. 122, 132002 (2019)

J/ψ

D⁰

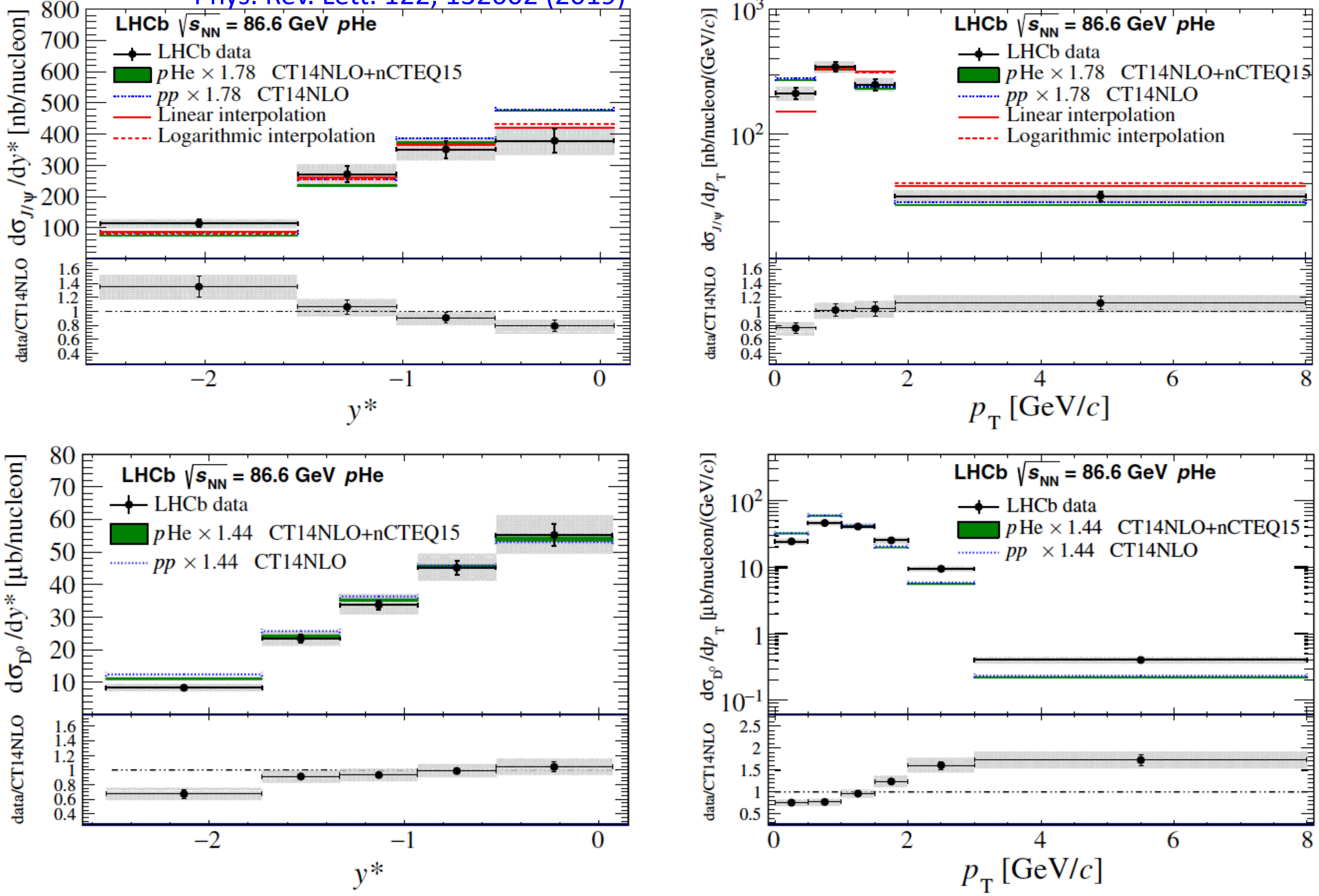

HELAC-ONIA predictions:
- JHEP 1303 (2013) 122
- Eur. Phys. J. C 77, 1 (2017)
- Comput. Phys. Commun. 198, 238 (2016)

Phenom. models:
- JHEP 1303 (2013) 122
- JHEP 05 (2013) 155

- HELAC-Onia calculations underestimate the data (scale factor needed)
- y^* dependence pretty well described, but p_T dependence not so well described
- Differential yields from p-Ar collisions at $\sqrt{s_{NN}} = 110$ GeV in back-up slides

Do we observe effects from intrinsic charm?

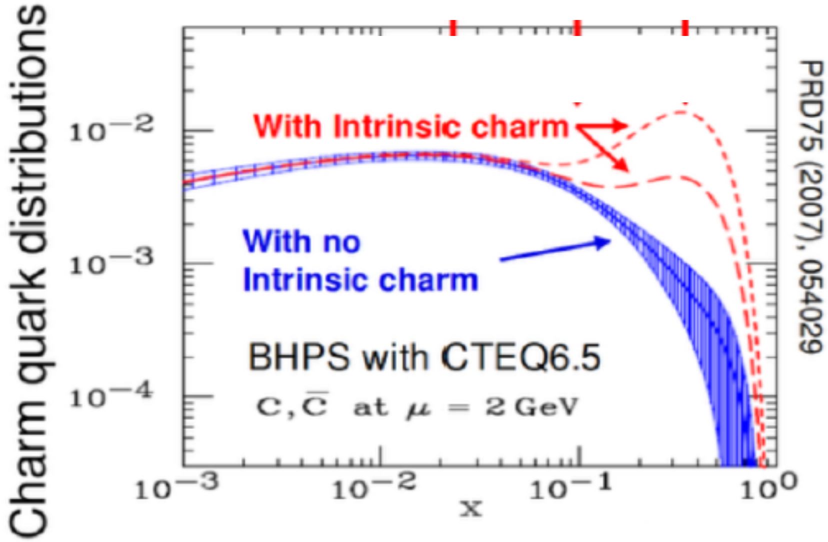

Do we observe effects from intrinsic charm?

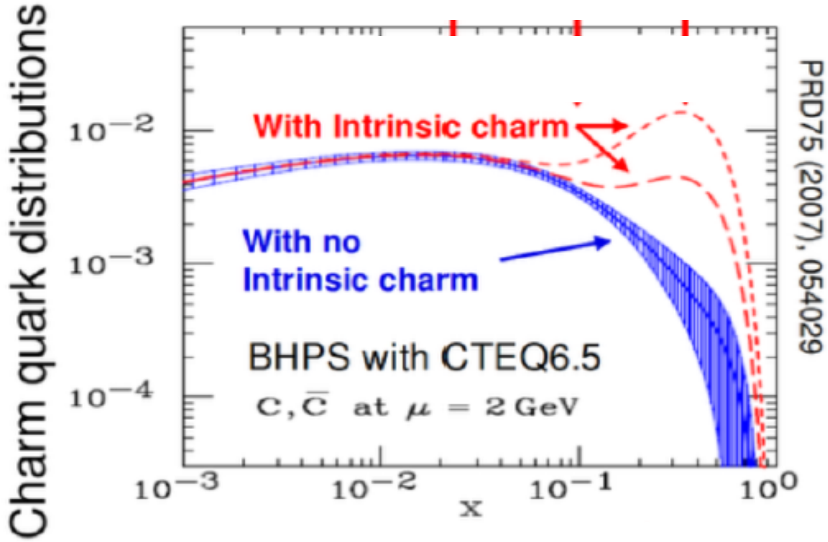

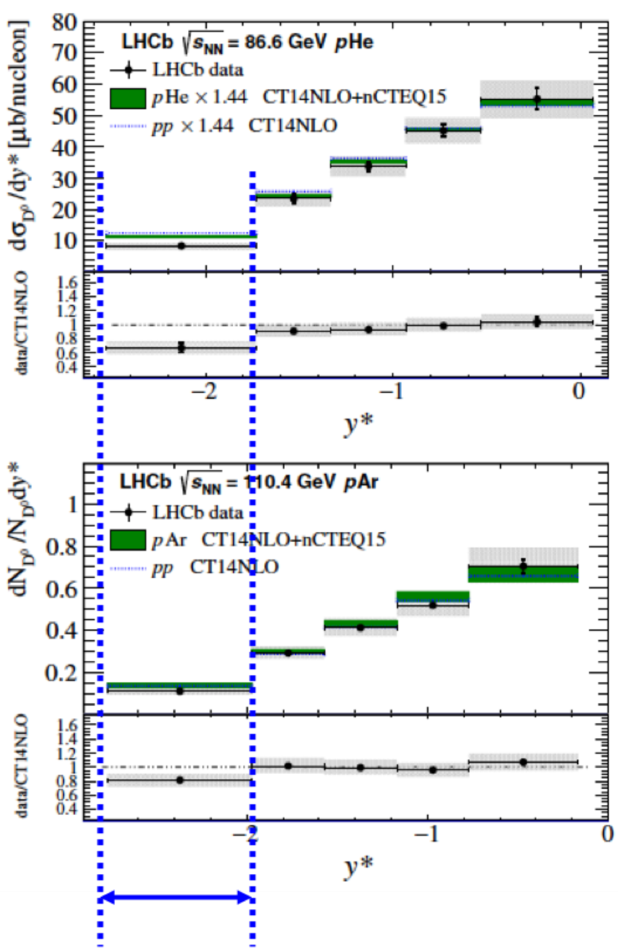

$$x \simeq \frac{2m_c}{\sqrt{s_{NN}}} e^{-y^*} \quad \Longrightarrow \quad high\, x \leftrightarrow y^* < 0$$

- The most backward bin corresponds to $x \in [0.17, 0.37]$

Do we observe effects from intrinsic charm?

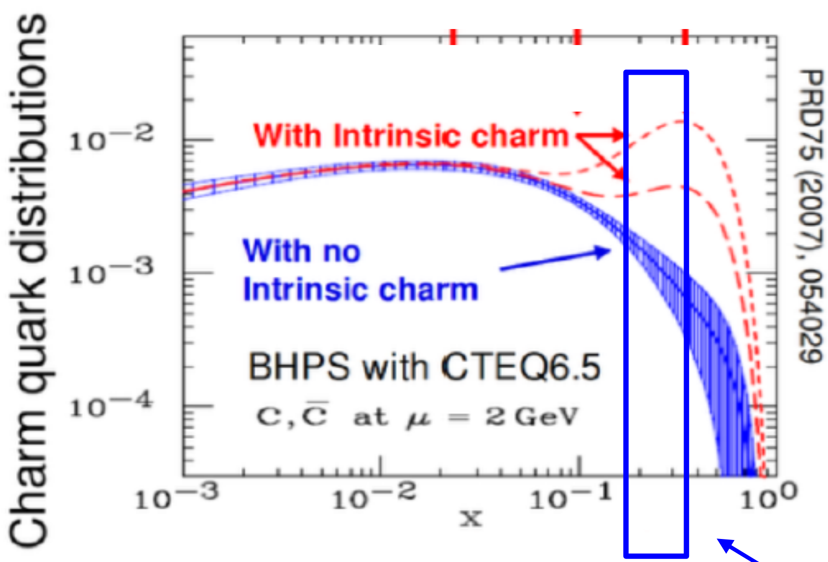

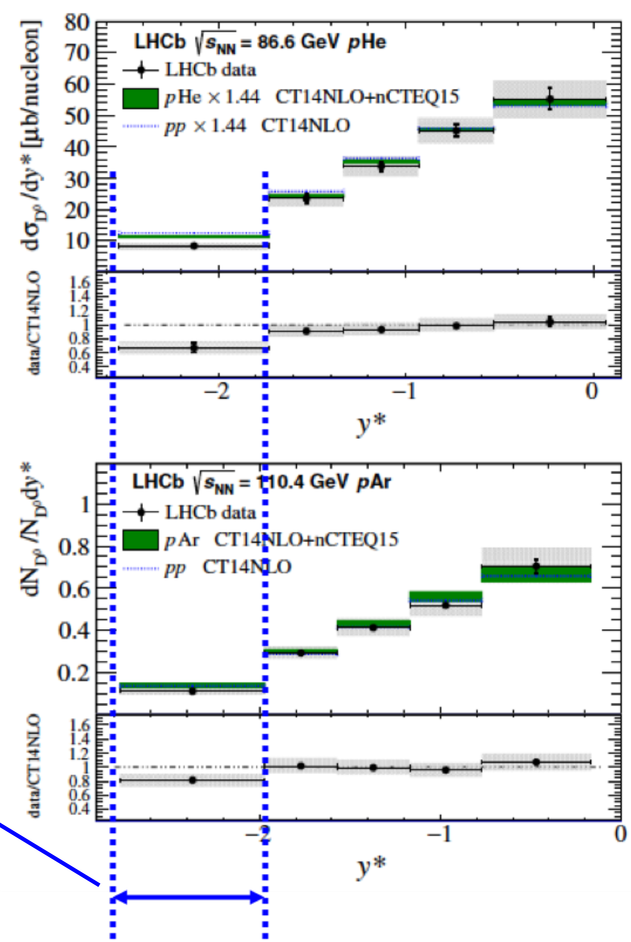

$$x \simeq \frac{2m_c}{\sqrt{s_{NN}}} e^{-y^*} \quad \Longrightarrow \quad high\, x \leftrightarrow y^* < 0$$

- The most backward bin corresponds to $x \in [0.17, 0.37]$
- In this range intrinsic charm is expected to contribute substantially
- No strong effect is seen by comparing pHe data with theoretical prediction which do not include any intrinsic charm contribution

First physics results with SMOG

- Antiproton production in p-He collisions

Antiproton production in p-He collisions at $\sqrt{s_{NN}} \sim 110$ GeV

The antiproton fraction in cosmic rays is a sensitive indirect probe for exotic astrophysical sources of antimatter, such as DM annihilation.

An excess of antiprotons over current predictions based on spallation of primary cosmic rays on interstellar medium (H and He) has been recently observed by the space-borne PAMELA and AMS-02 experiments.

However, present predictions for $\bar{p}/p$ flux ratio from the known production sources are limited by large uncertainties on $\bar{p}$ production cross sections (especially from He).

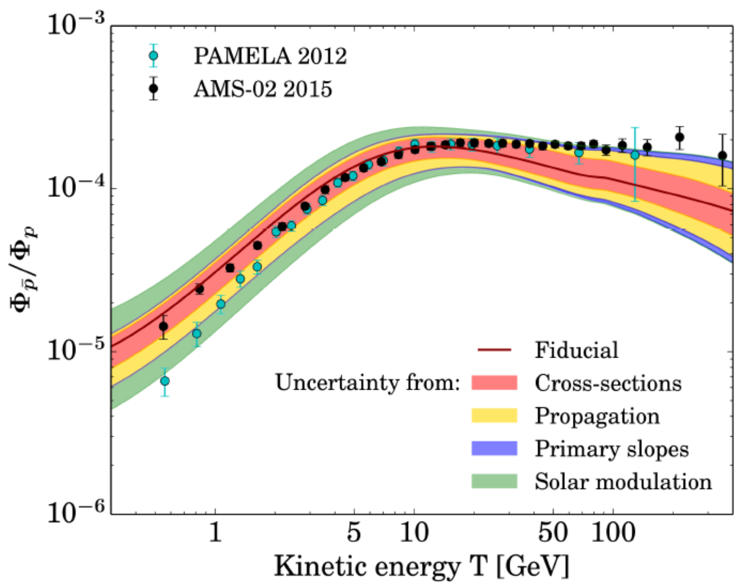

Antiproton production in p-He collisions at $\sqrt{s_{NN}} \sim 110$ GeV

The antiproton fraction in cosmic rays is a sensitive indirect probe for exotic astrophysical sources of antimatter, such as DM annihilation.

An excess of antiprotons over current predictions based on spallation of primary cosmic rays on interstellar medium (H and He) has been recently observed by the space-borne PAMELA and AMS-02 experiments.

However, present predictions for $\bar{p}/p$ flux ratio from the known production sources are limited by large uncertainties on $\bar{p}$ production cross sections (especially from He).

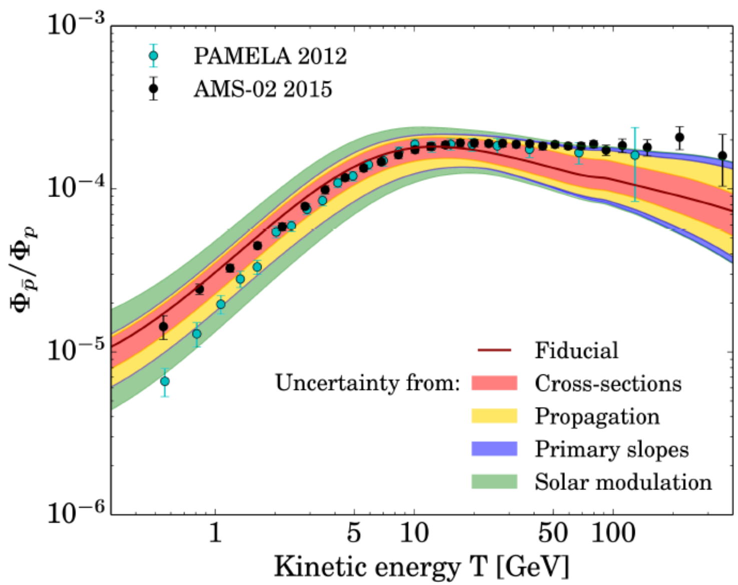

- LHCb has provided the **first direct measurement of $\bar{p}$ production in fixed-target p-He collisions**.

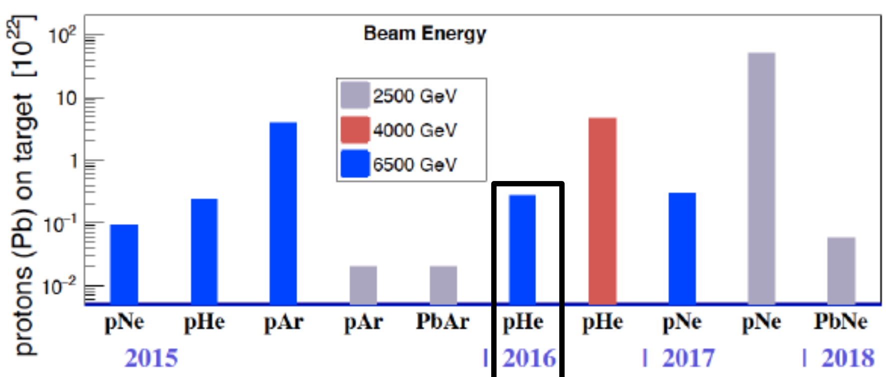

$\sqrt{s_{NN}} = 110$ GeV

Antiproton production in p-He collisions at $\sqrt{s_{NN}} \sim 110$ GeV

$\bar{p}$ with momentum in the range 12-100 GeV/c
are clearly identified by the two RICH detectors

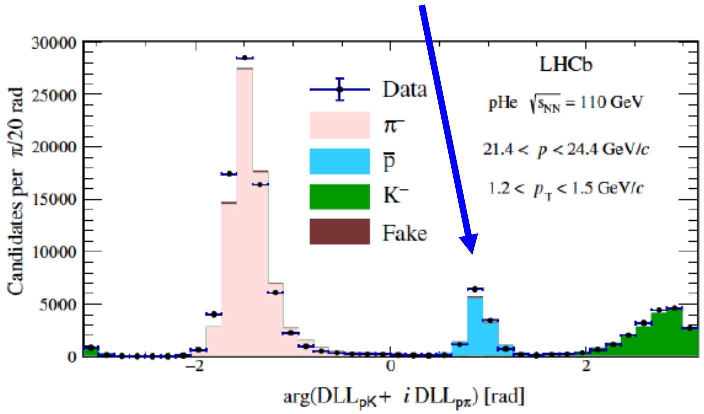

Antiproton production in p-He collisions at $\sqrt{s_{NN}} \sim 110$ GeV

$\bar{p}$ with momentum in the range 12-100 GeV/c are clearly identified by the two RICH detectors

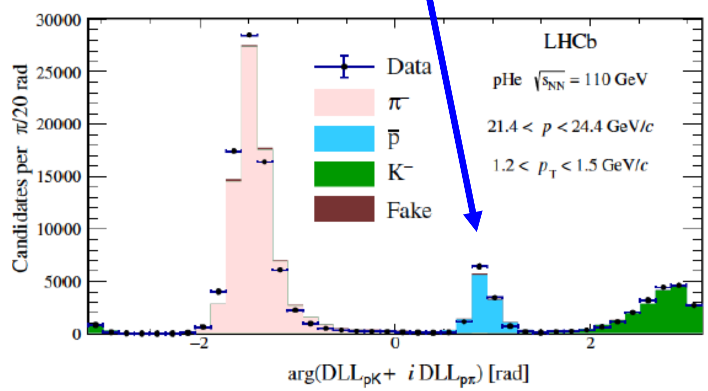

Phys. Rev. Lett. 121, 222001 (2018)

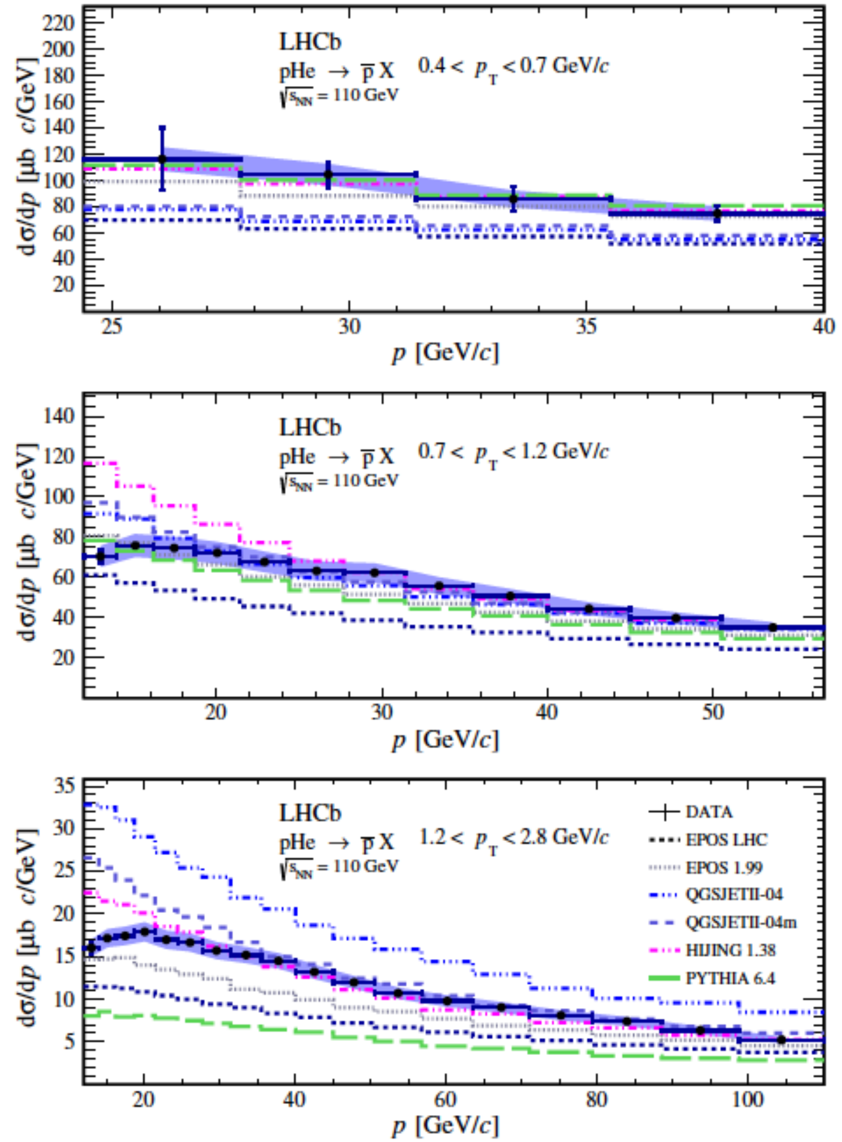

- Comparison of the result with MC generators:

- EPOS LHC
- EPOS 1.99
- QGSJET-II-04
- QGSJETII-04m
- HIJING 1.34
- PYTHIA 6.4

Error bars significantly smaller than predictions spread!

SMOG2 the upgraded SMOG system

The SMOG2 setup

The upgraded SMOG system (SMOG2) is based on the use of a storage cell for the target gas

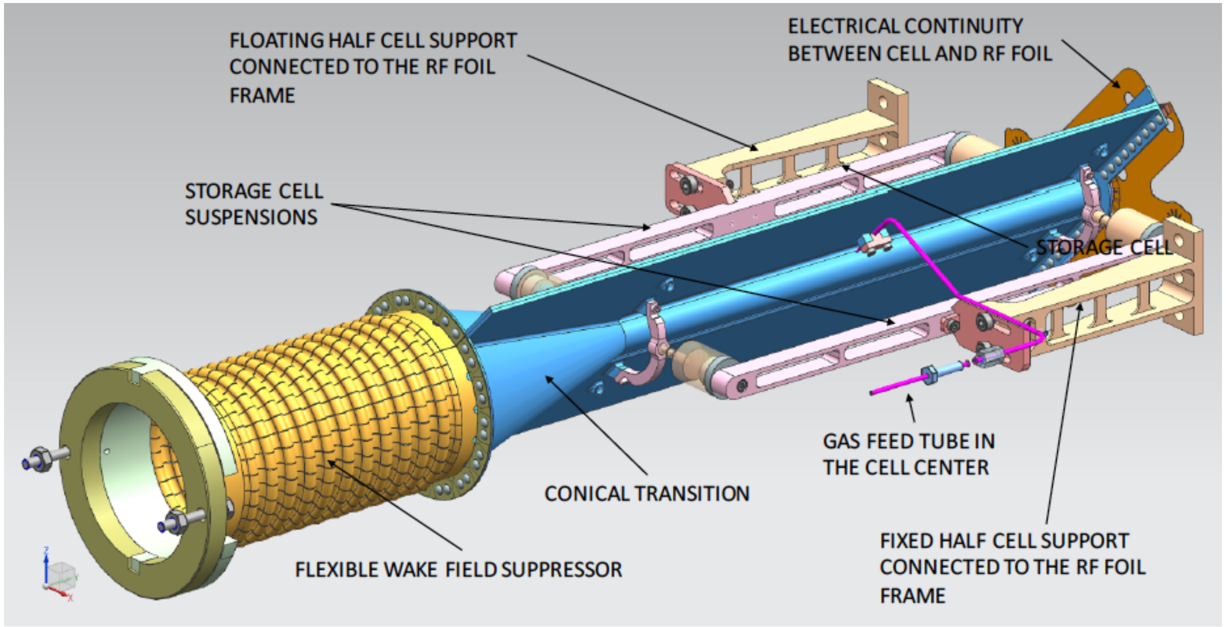

The SMOG2 setup

The upgraded SMOG system (SMOG2) is based on the use of a storage cell for the target gas

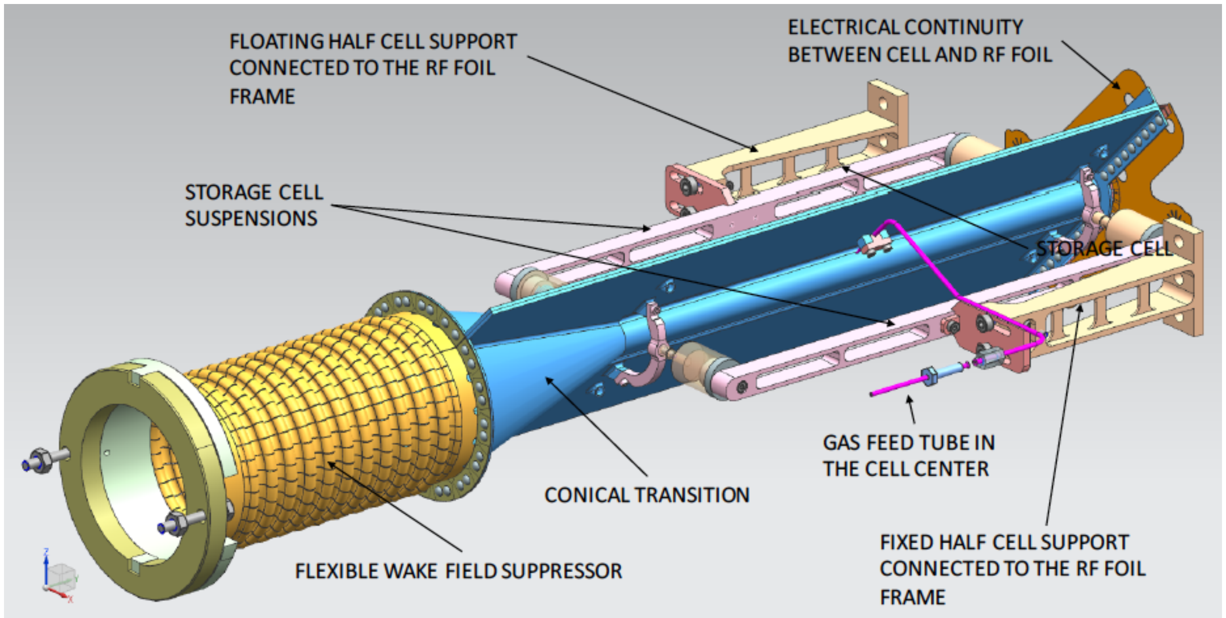

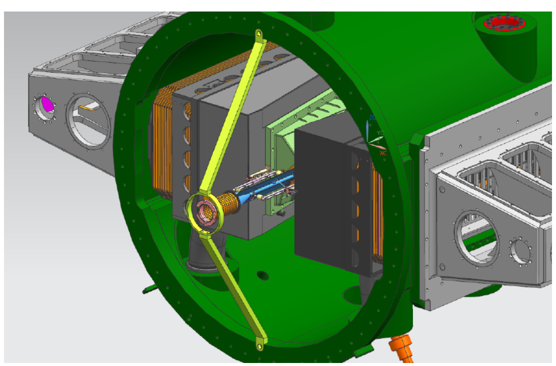

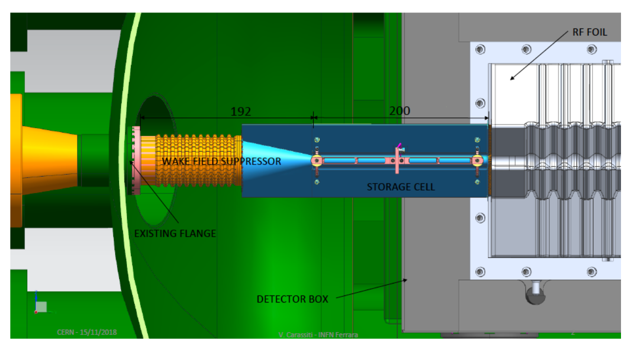

SMOG2 vs. SMOG

- ✓ **Increase of target density (luminosity)** by up to 2 orders of magnitude using the same gas load of SMOG ($\sim 10^{-7}$ mbar)
- ✓ Possibility to inject **more gas species**: H, D, He, N, O, Ne, Ar, Kr, Xe (SMOG: He, Ne, Ar)
- ✓ **More sophisticated Gas Feed System**: will allow to measure the target density (and luminosity) with much higher precision.
- ✓ Well **defined interaction region** upstream of the collider IP (limited to cell length: 20 cm)
- ✓ SMOG2 can (in principle) **run in parallel with collider mode** (well displaced IP)

…More details on expected performances in back-up slides

SMOG2 vs. SMOG

- ✓ **Increase of target density (luminosity)** by up to 2 orders of magnitude using the same gas load of SMOG ($\sim 10^{-7}$ mbar)
- ✓ Possibility to inject **more gas species**: H, D, He, N, O, Ne, Ar, Kr, Xe (SMOG: He, Ne, Ar)
- ✓ **More sophisticated Gas Feed System**: will allow to measure the target density (and luminosity) with much higher precision.
- ✓ Well **defined interaction region** upstream of the collider IP (limited to cell length: 20 cm)
- ✓ SMOG2 can (in principle) **run in parallel with collider mode** (well displaced IP)

…More details on expected performances in back-up slides

- ✓ **Installation scheduled for November 2019 (during LHC LS2)**
- ✓ **Data taking will start in 2021 (LHC Run3)**

Selected physics opportunities with SMOG2

Opportunities with SMOG2: heavy-ion physics

- New measurements of prompt charm production with a significantly increased statistical power. New measurements can include also **charmed baryons** (e.g. Λ_c^+).

Opportunities with SMOG2: heavy-ion physics

- New measurements of prompt charm production with a significantly increased statistical power. New measurements can include also **charmed baryons** (e.g. Λ_c^+).
- Measurements can be extended to charmonium excited states. Relevant for studying the **sequential charmonia suppression**

arXiv:hep-ph/0512217

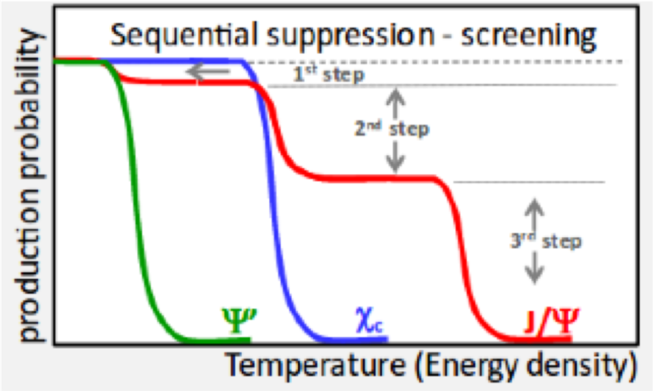

(different binding energies lead to different dissociation temperatures)

Opportunities with SMOG2: heavy-ion physics

- New measurements of prompt charm production with a significantly increased statistical power. New measurements can include also **charmed baryons** (e.g. Λ_c^+).
- Measurements can be extended to charmonium excited states. Relevant for studying the **sequential charmonia suppression**

arXiv:hep-ph/0512217

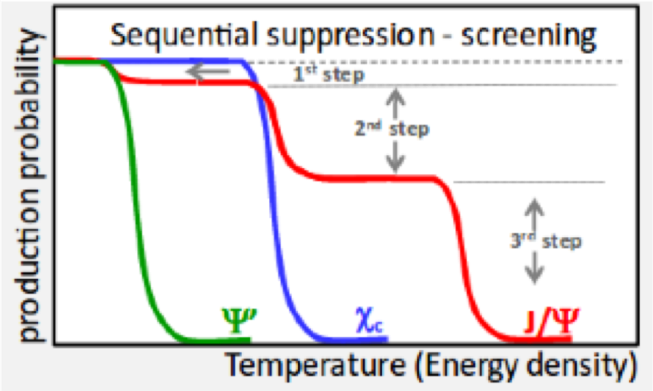

(different binding energies lead to different dissociation temperatures)

- Possibility to measure **prompt beauty production** (7k reconstrcuted $\Upsilon(1S) \rightarrow \mu^+\mu^-$ events are foreseen with $\mathcal{L} \sim 45\ pb^{-1}$ in pAr collisions)

Opportunities with SMOG2: heavy-ion physics

- New measurements of prompt charm production with a significantly increased statistical power. New measurements can include also **charmed baryons** (e.g. Λ_c^+).
- Measurements can be extended to charmonium excited states. Relevant for studying the **sequential charmonia suppression**

arXiv:hep-ph/0512217

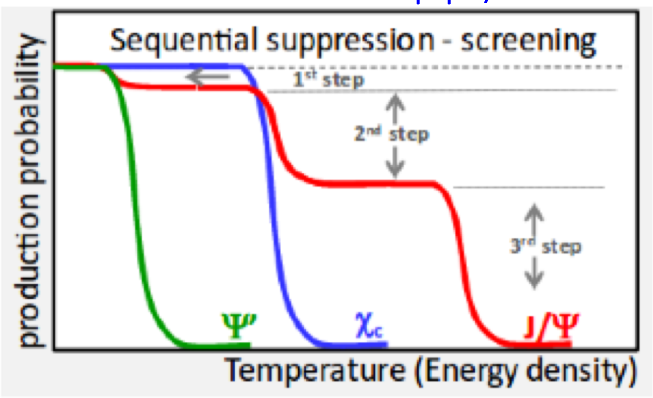

(different binding energies lead to different dissociation temperatures)

- Possibility to measure **prompt beauty production** (7k reconstructed $\Upsilon(1S) \rightarrow \mu^+\mu^-$ events are foreseen with $\mathcal{L} \sim 45\ pb^{-1}$ in pAr collisions)
- Measurement of QGP-related flow observables and correlations in Pb-A collisions at $\sqrt{s_{NN}} \sim 70$ GeV

Opportunities with SMOG2: cosmic rays and DM

- Extend the present antiproton production measurement to include **production of antiprotons from anti-hyperon decays (e.g., $\overline{\Lambda}, \overline{\Sigma}$)**

Opportunities with SMOG2: cosmic rays and DM

- Extend the present antiproton production measurement to include **production of antiprotons from anti-hyperon decays (e.g., $\overline{\Lambda}, \overline{\Sigma}$)**

- Thanks to the possibility to use also a H_2 target, it will be possible to precisely measure the ratio:

$$\frac{\sigma(pHe \to \bar{p}X)}{\sigma(pH \to \bar{p}X)}$$

where many systematic uncertainties cancel

Opportunities with SMOG2: cosmic rays and DM

- Extend the present antiproton production measurement to include **production of antiprotons from anti-hyperon decays (e.g., $\overline{\Lambda}, \overline{\Sigma}$)**

- Thanks to the possibility to use also a H_2 target, it will be possible to precisely measure the ratio:

$$\frac{\sigma(pHe \to \bar{p}X)}{\sigma(pH \to \bar{p}X)}$$

where many systematic uncertainties cancel

- Explore the possibility to measure **production of light anti-nuclei ($\overline{d}$, $\overline{^{3}He}$, $\overline{^{4}He}$)**

Opportunities with SMOG2: nucleon structure

- SMOG2 operated with H_2 and D_2 targets offers unique conditions to probe quark and gluon PDFs in nucleons and nuclei, especially at high-x and moderately-high Q^2, where present experimental data are largely insufficient to constraint the theoretical distributions.

Opportunities with SMOG2: nucleon structure

- SMOG2 operated with H_2 and D_2 targets offers unique conditions to probe quark and gluon PDFs in nucleons and nuclei, especially at high-x and moderately-high Q^2, where present experimental data are largely insufficient to constraint the theoretical distributions.

- Measurements of **quark and gluon transverse-momentum-dependent (TMD) PDFs**, respectively in Drell-Yan and inclusive production of quarkonia (J/ψ, ψ', Υ, etc.), will significantly improve our understanding of the 3D structure of the nucleon in the non-perturbative regime of QCD.

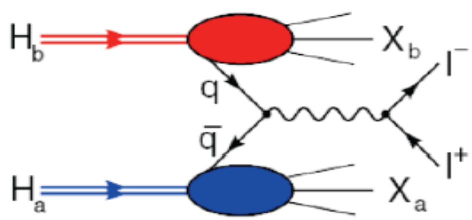

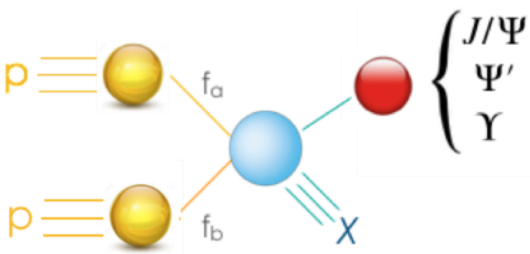

… More details in back-up slides

Conclusions

- LHCb is presently the only LHC experiment that can run in both collider and fixed-target mode.

- The SMOG system has been successfully exploited for interesting fixed-target physics:

- **prompt charm production in p-He and pAr collisions** (cold nuclear-matter studies and baseline measurements for QGP related studies)
- **antiproton production in p-He collisions** (cosmic rays physics and DM search)
- Other analyses are ongoing

Conclusions

- LHCb is presently the only LHC experiment that can run in both collider and fixed-target mode.

- The SMOG system has been successfully exploited for interesting fixed-target physics:

- **prompt charm production in p-He and pAr collisions** (cold nuclear-matter studies and baseline measurements for QGP related studies)
- **antiproton production in p-He collisions** (cosmic rays physics and DM search)
- Other analyses are ongoing

- The **upgraded SMOG system (SMOG2)**, based on the use of a storage cell for the target gas to be installed by the end of 2019, will significantly enhance the performances of fixed-target physics at LHCb and will allow for a broad and ambitious physics program.

Back-up

Prompt charm production in p-Ar collisions at $\sqrt{s} = 110$ GeV

Phys. Rev. Lett. 122, 132002 (2019)

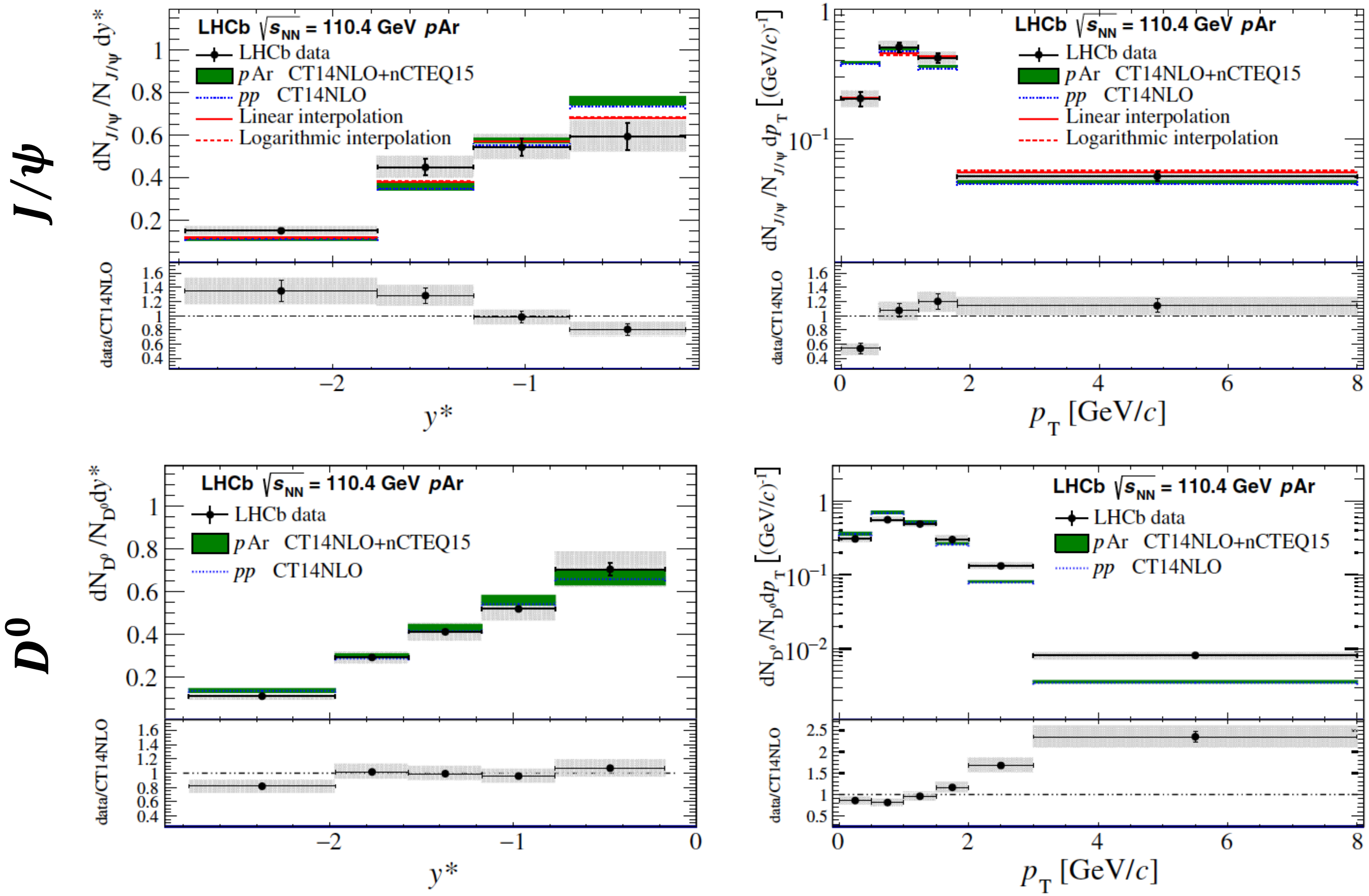

HELAC-ONIA predictions:
- JHEP 1303 (2013) 122
- Eur. Phys. J. C 77, 1 (2017)
- Comput. Phys. Commun. 198, 238 (2016)

Phenom. models:
- JHEP 1303 (2013) 122
- JHEP 05 (2013) 155

➢ y^* dependence pretty well described, but p_T dependence not so well described

Antiproton production in p-He collisions at $\sqrt{s_{NN}} \sim 110$ GeV

The **Integrated luminosity ($484 \pm 7 \pm 29\ \mu b^{-1}$)** was determined from the yield of atomic electrons from elastic scattering the proton beam:

- Since the main background processes are charge-symmetric (i.e. produce same amount of e^+ and e^- candidates), the background yield is determined from events with a single e^+ candidate.

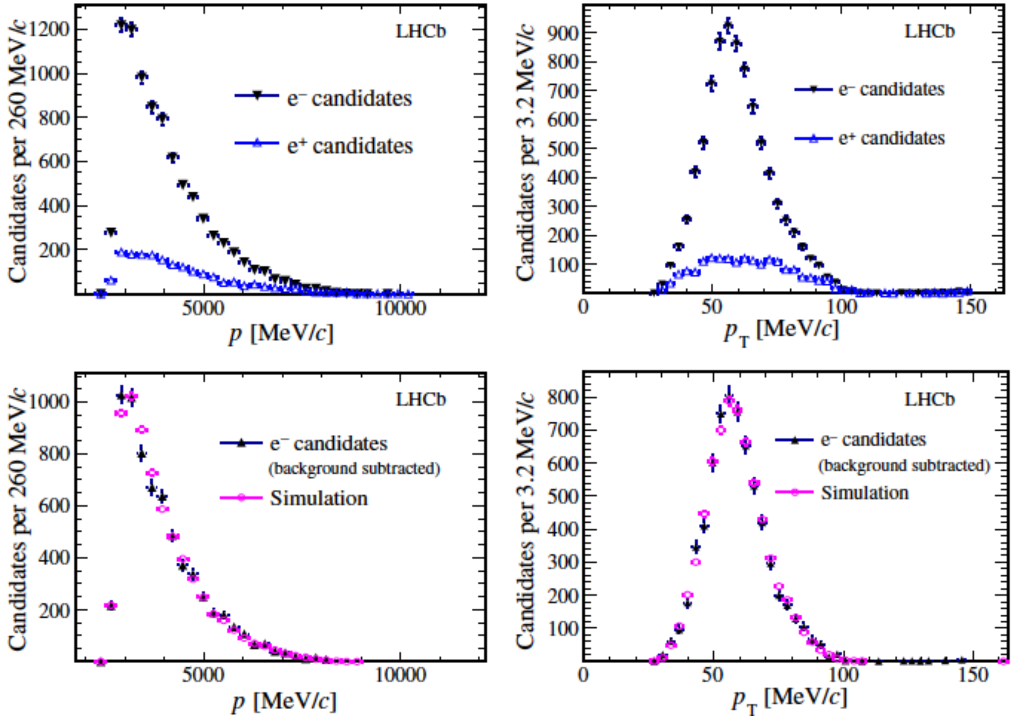

- background is further suppressed by two multivariate classifiers based on BDT
- Total systematic uncertainty on luminosity is 6.0%

The SMOG2 setup

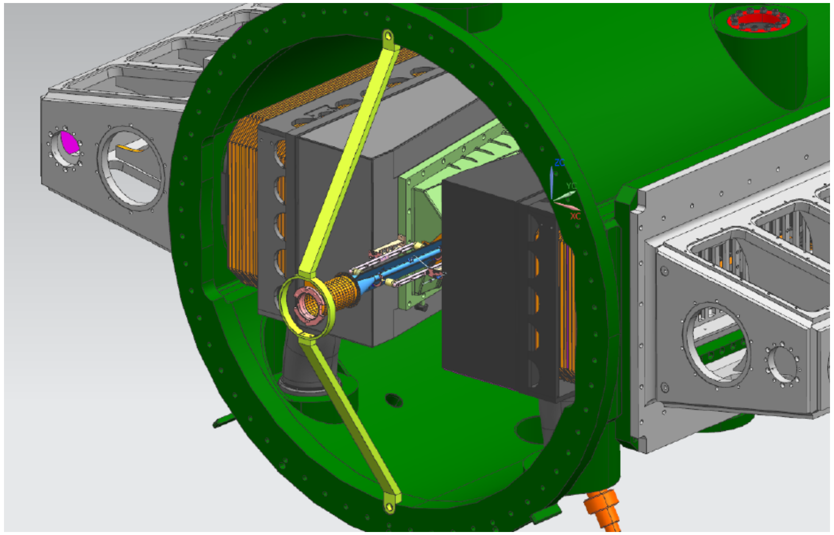

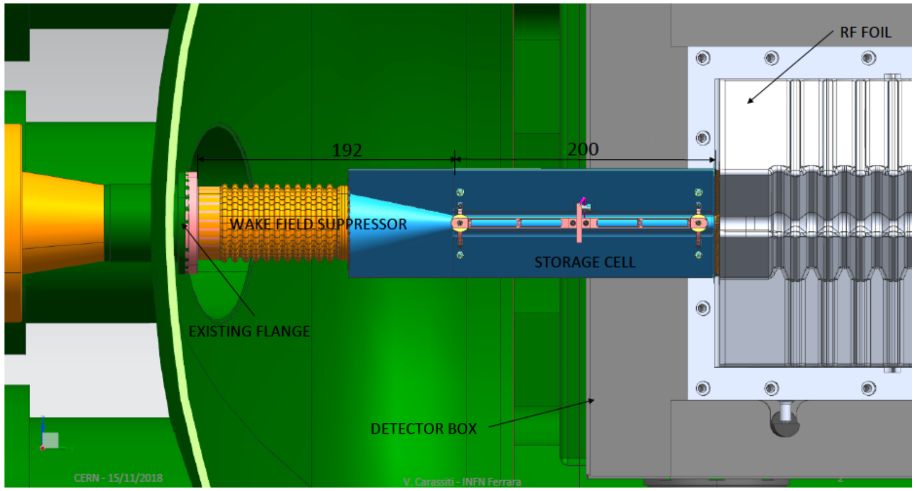

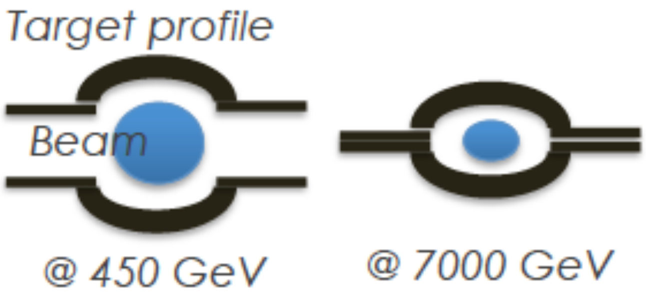

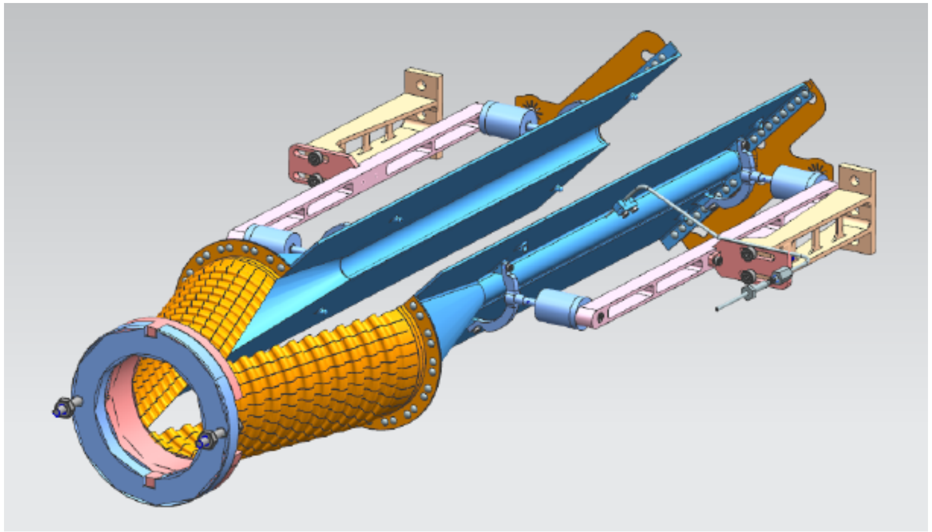

The SMOG2 setup

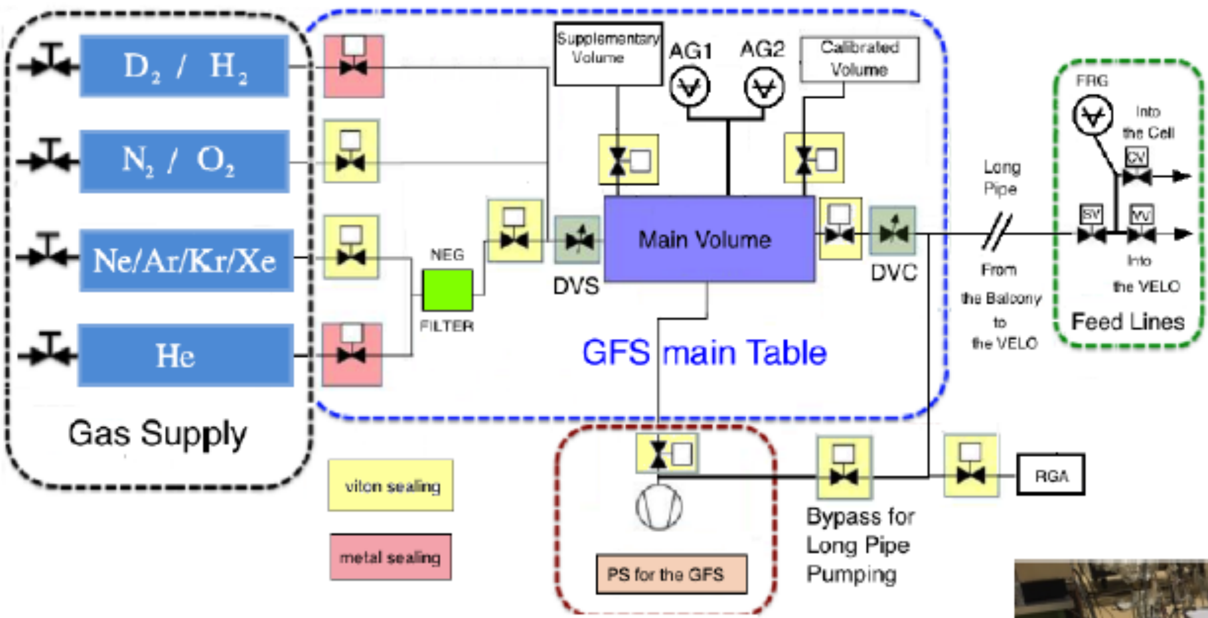

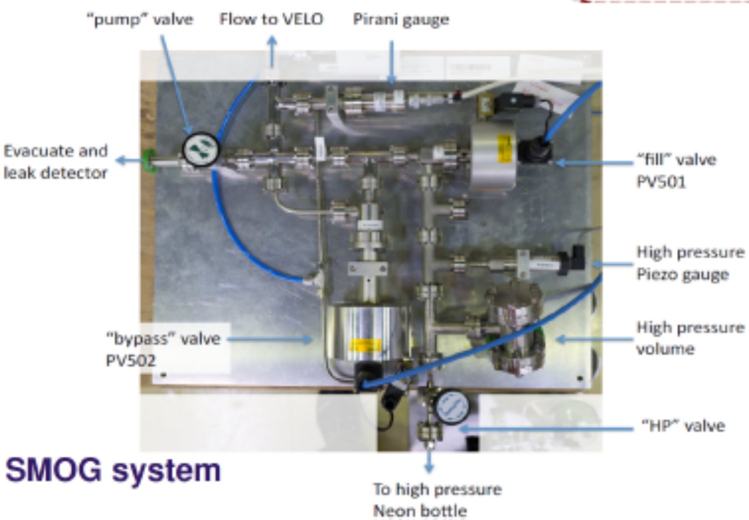

SMOG system

SMOG2 Gas Feed System
(under construction)

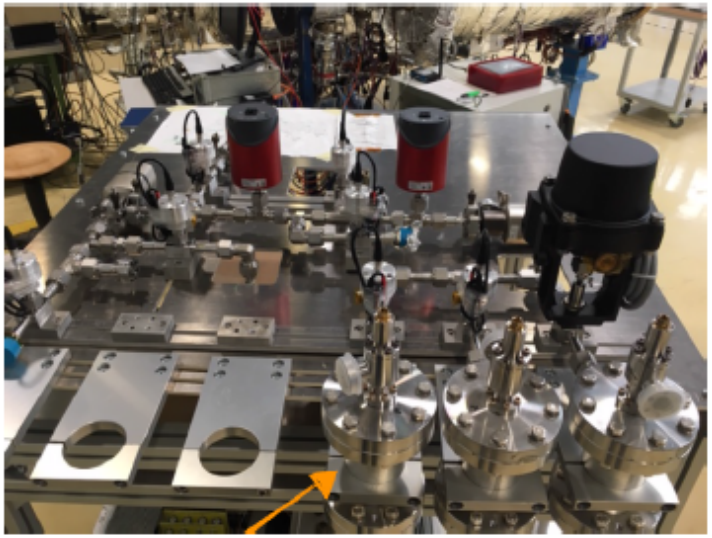

SMOG2 projected performances for LHC Run3

System	$\sqrt{s_{NN}}$ (GeV)	< pressure> (10^{-5} mbar)	ρ_S (cm^{-2})	$\mathcal{L}$ ($\mathrm{cm}^{-2}\mathrm{s}^{-1}$)	Rate (MHz)	Time (s)	$\int\mathcal{L}$ (pb^{-1})
$p\mathrm{H}_2$	115	4.0	2.0×10^{13}	6×10^{31}	4.6	2.5×10^{6}	150
$p\mathrm{D}_2$	115	2.0	1.0×10^{13}	3×10^{31}	4.3	0.3×10^{6}	9
$p\mathrm{Ar}$	115	1.2	0.6×10^{13}	1.8×10^{31}	11	2.5×10^{6}	45
$p\mathrm{Kr}$	115	0.8	0.4×10^{13}	1.2×10^{31}	12	2.5×10^{6}	30
$p\mathrm{Xe}$	115	0.6	0.3×10^{13}	0.9×10^{31}	12	2.5×10^{6}	22
$p\mathrm{He}$	115	2.0	1.0×10^{13}	3×10^{31}	3.5	3.3×10^{3}	0.1
$p\mathrm{Ne}$	115	2.0	1.0×10^{13}	3×10^{31}	12	3.3×10^{3}	0.1
$p\mathrm{N}_2$	115	1.0	0.5×10^{13}	1.5×10^{31}	9.0	3.3×10^{3}	0.1
$p\mathrm{O}_2$	115	1.0	0.5×10^{13}	1.5×10^{31}	10	3.3×10^{3}	0.1
PbAr	72	8.0	4.0×10^{13}	1×10^{29}	0.3	6×10^{5}	0.060
PbH_2	72	8.0	4.0×10^{13}	1×10^{29}	0.2	1×10^{5}	0.010
$p\mathrm{Ar}$	72	1.2	0.6×10^{13}	1.8×10^{31}	11	3×10^{5}	5

Assumptions:

- Parallel beam-gas and beam-beam data taking for $1/3$ of total beam time
- Use of all beam bunches for fixed-target physics
- Beam intensity of 2.6×10^{14} protons (2.2×10^{11} Pb ions)

SMOG2 projected performances for LHC Run3

E.g. for **p-Ar collisions**

	SMOG published result pHe@87 GeV	SMOG largest sample pNe@69 GeV	SMOG2 example pAr@115 GeV
Integrated luminosity	7.6 nb^{-1}	$\sim$ 100 nb^{-1}	$\sim$ 45 pb^{-1}
syst. error on J/ψ x-sec.	7%	6 - 7%	2 - 3 %
J/ψ yield	400	15k	15M
D^0 yield	2000	100k	150M
Λ_c^+ yield	20	1k	1.5M
$\psi(2S)$ yield	negl.	150	150k
$\Upsilon(1S)$ yield	negl.	4	7k
Low-mass Drell-Yan yield	negl.	5	9k

Assumptions:

- Parallel beam-gas and beam-beam data taking for 1/3 of total beam time
- Use of all beam bunches for fixed-target physcs
- Beam intensity of 2.6×10^{14} protons (2.2×10^{11} Pb ions)

SMOG2 vs. SMOG

Reaction	DAQ time	Non coll. bunches	Lumi (nb^{-1})	Decays	SMOG yields	Scale factor	SMOG2 proj. yields
pAr	18 h	684	~ 2	$D^0 \to K^-\pi^+$	6450	62	400 k
				$D^+ \to K^-\pi^+\pi^+$	975		60 k
				$D_s^+ \to K^-K^+\pi^+$	131		8 k
				$D^{*+} \to D^0\pi^+$	2300		140 k
				$\Lambda_c^+ \to pK^-\pi^+$	50		3 k
				$J/\psi \to \mu^+\mu^-$	500		30 k
				$\psi(2S) \to \mu^+\mu^-$	20		1.2 k
pHe	84 h	648	7.6	$J/\psi \to \mu^+\mu^-$	500	19.6	10 k
				$\psi(2S) \to \mu^+\mu^-$	20		0.4 k

Assumptions:

- PV region of 40 cm ($-500\ mm < z_{PV} < -100$ mm)
- Same data taking periods for SMOG and SMOG2 with only non-colliding proton bunches
- Global reconstruction efficiencies 10% lower for SMOG2

The quark TMDs

		Quark TMDs		
		U	L	T
Hadron	U	f_1		$h_1^\perp$
	L		g_1	$h_{1L}^\perp$
	T	$f_{1T}^\perp$	$g_{1T}^\perp$	h_1, $h_{1T}^\perp$

- **8 independent TMDs at twist-2**
- **Each with a probabilistic interpretation in terms of parton densities**
- **Significant experimental progress in the last 15 years!**
- First extractions from global analyses

- So far, main results obtained in **SIDIS** measurements (HERMES, COMPASS, JLAB)
- **Drell-Yan** in hadron-hadron collisions represents a complementary approach
- Unique kinematic region with fixed-target collisions at LHC
- Comparison of results from SIDIS and DY will allow to set stringent tests on QCD: factorization, evolution, universality

Mapping the nucleon structure …and more

Collinear PDFs

1D

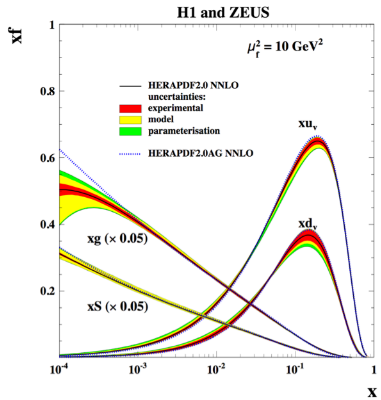

electroencephalograms

1D

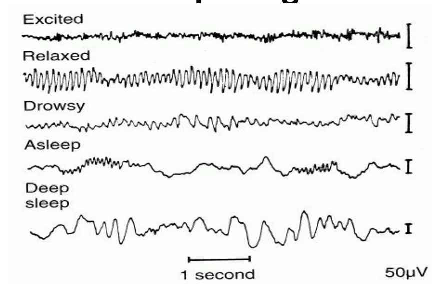

TMDs

3D

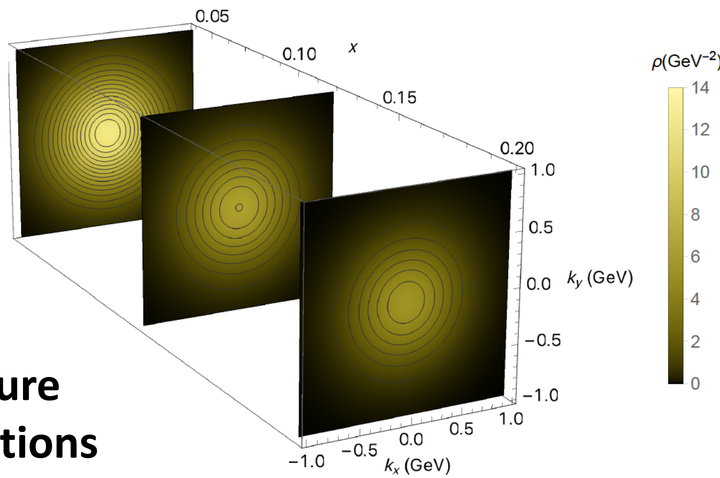

(Courtesy of A. Bacchetta)

3D **NMR imaging**

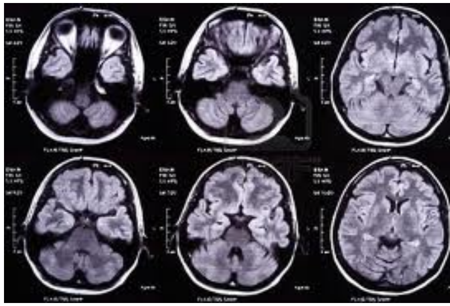

- **3D maps of nucleon structure**
- **Describe spin-orbit correlations**
- **Are sensitive to the parton OAM**
- **T-odd TMDs are process dependent**

(breaking of QCD universality! ..see details in backup slides**)**

Probing the quark TMDs with fixed-targets at LHC

Unpolarized Drell-Yan

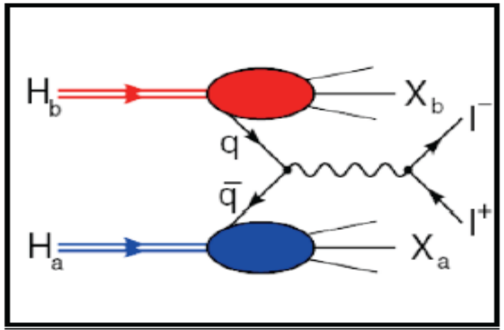

- Clean process
- LHC experiments have excellent reconstruction capabilities for $\mu\mu$ channel!

- Dominant process: $\bar{q}(x_{beam}) + q(x_{target}) \rightarrow \mu\mu$

- **Provides sensitivity to unpolarized and BM TMDs**

$$\sigma_{UU} \quad \propto \quad f_1 f_1 + \cos 2\phi\, h_1^{\perp} h_1^{\perp}$$

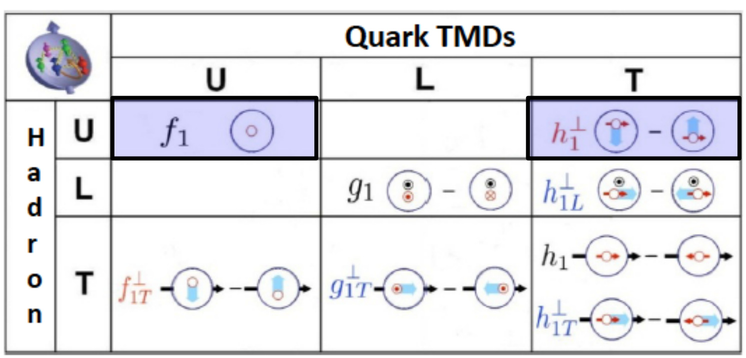

- Using fixed H and D targets allows to study the **antiquark content of the nucleon!**

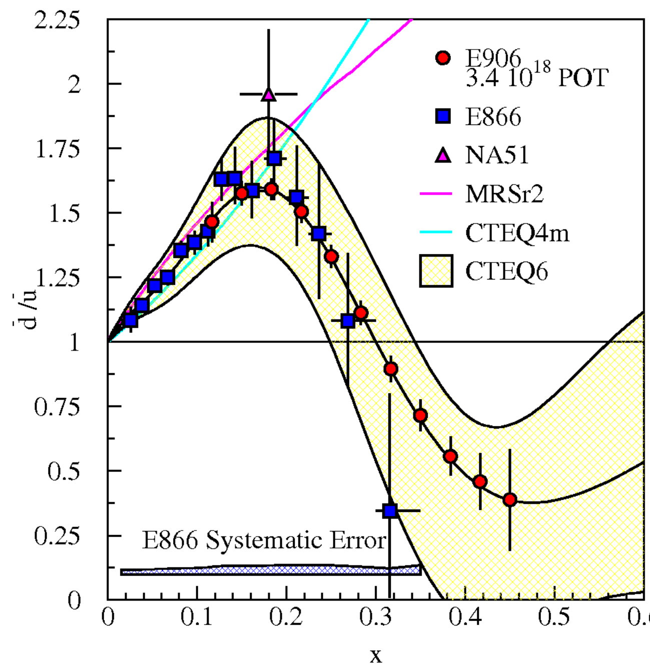

$\bar{d}(x) \neq \bar{u}(x)$!!

- hints that: $\bar{s}(x) \neq s\,(x)$
- **sea is not flavour symmetric!**
- **intrinsic sea quarks**?

Probing the gluon TMDs with fixed-targets at LHC

		Gluon TMDs		
		Unpol	Circularly pol.	Linearly pol.
Hadron	U	f_1^g		$h_1^{\perp g}$
	L		g_1^g	$h_{1L}^{\perp g}$
	T	$f_{1T}^{\perp g}$	$g_{1T}^{\perp g}$	h_{1T}^g $h_{1T}^{\perp g}$

Theory framework consolidated

...but experimental access still extremely limited!

Note: gluons with non-zero p_T inside an unpolarized hadron can be linearly polarized!

Probing the gluon TMDs with fixed-targets at LHC

In high-energy hadron collisions Heavy quarks dominantly produced through gg interactions:

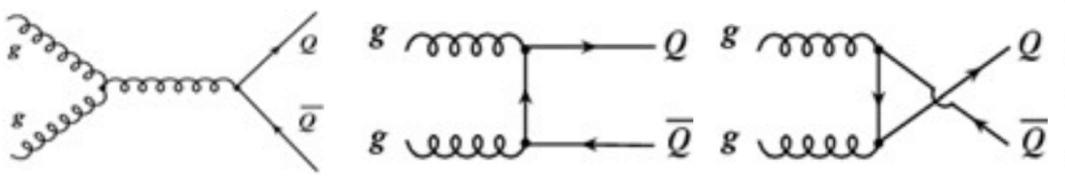

The most efficient way to access the gluon dynamics inside the proton at LHC is to **measure heavy-flavour observables**

Inclusive quarkonia production in pp interaction turns out to be an ideal **gluon-sensitive observable!**

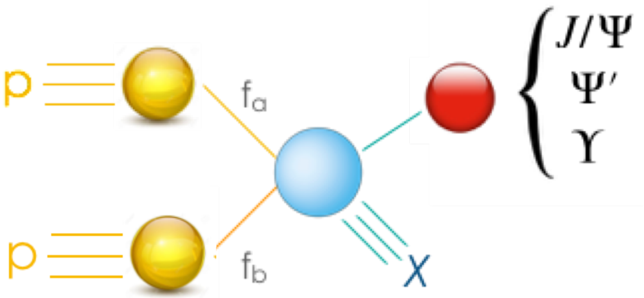

Opportunities with SMOG2: nucleon structure

SMOG2 operated with H_2 and D_2 targets offers unique conditions to probe quark and gluon PDFs in nucleons and nuclei, especially at high-x and moderately-high Q^2, where present experimental data are insufficient to constraint the theoretical distributions.

- Measure of **transverse momentum dependent quark PDFs** f_1^q and $h_1^{\perp q}$ in Drell-Yan processes by exploiting the azimuthal dependence of the **unpolarized DY cross section**:

$$\sigma_{DY} \propto A f_1^q \otimes f_1^q + B h_1^{\perp q} \otimes h_1^{\perp q} \cos 2\phi$$

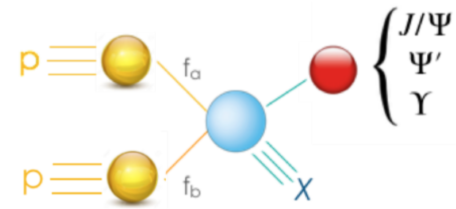

- Access to still unmeasured **transverse momentum dependent gluon PDFs** f_1^g and $h_1^{\perp g}$ in **inclusive production of quarkonia states** (J/ψ, ψ', Υ, etc.) by exploiting the azimuthal dependence of the cross section:

$$\sigma_{incl\ Q\bar{Q}} \propto A f_1^g \otimes f_1^g + B f_1^g \otimes h_1^{\perp g} \cos 2\phi + C h_1^{\perp g} \otimes h_1^{\perp g} \cos 4\phi$$

- Measure antiquark PDFs ($\bar{u}(x), \bar{d}(x)$) in DY processes. Test of flavor dependence of the the proton sea.